Towards early-stage facade design for heat resilient buildings: impact of weather file generation for office buildings in temperate climates

Building and Environment 284 (2025) 113459

Contents lists available at ScienceDirect

Building and Environment

journal homepage: www.elsevier.com/locate/buildenv

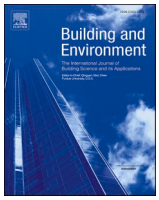

Towards early-stage facade design for heat resilient buildings: impact of weather file generation for office buildings in temperate climates

Milad Heiranipour [a,b,c], Miren Juaristi [b], Stefano Avesani [b], Fabio Favoino [a,*]

[a] Technology Energy Building Environment (TEBE) Research Group, Energy Department, Politecnico di Torino, Corso Duca degli Abruzzi 24, Turin, Italy
[b] EURAC Research, Institute for Renewable Energy, Viale Druso 1, I-39100, Bolzano, Italy
[c] Scuola Universitaria Superiore IUSS Pavia, Italy

ARTICLE INFO

Keywords:
Building envelope performance
Building heat resilience
Downscaling methods
Future weather files
Sensitivity analysis

ABSTRACT

This study examines how different approaches to generating Future Typical Meteorological Year (F-TMY) data influence both absolute performance predictions and comparative evaluation of early-stage façade design strategies. The analysis compares three weather file generation methods - dynamical downscaling through Regional Climate Models (RCM) and two statistical approaches (morphing implemented through CCWeatherGen and stochastic modelling implemented through Meteonorm) – to assess their impact on building thermal resilience predictions across three-time horizons (2020, 2050, 2080). Using a case study office building in the temperate climate of Turin, Italy, multiple thermal resilience indicators are evaluated, including energy use intensity, peak loads, indoor overheating degree, and heat release to the urban environment. The results reveal significant differences in absolute projections between the methods. For indoor overheating risk, CCWeatherGen projections exceed those of RCM by 300 % by 2080, indicating substantially different predictions of occupant thermal discomfort. In terms of peak cooling loads, RCM projects values 40 % higher than CCWeatherGen, while Meteonorm shows projections 70 % lower than CCWeatherGen by 2080, highlighting major discrepancies in system sizing requirements. For heat release to the urban environment, Meteonorm projections exceed RCM by 5 % in the future period, suggesting different implications for urban heat island mitigation strategies. These differences highlight significant methodological differences in predicting future building performance, especially for extreme conditions. However, despite these absolute differences, the comparative ranking of building envelope design strategies remains relatively consistent across methods. The analysis also reveals important trade-offs between performance objectives. For example, increasing the window-to-wall ratio up to 75 % produces opposing effects - reducing energy consumption through improved daylighting but significantly increasing the risk of overheating (48–56 % increase). These findings have significant implications for architectural practice and building performance modelling. While absolute performance predictions vary substantially between methods, the consistent ranking of design strategies provides reliable guidance for early-stage design decisions. Solar control measures emerge as the most effective strategy across all methods, offering designers confidence in prioritizing these elements regardless of climate data methodology. This research provides practical guidance for integrating climate adaptation into façade design while managing the inherent uncertainties in future climate projections.

Abbreviations: BPS, Building Performance Simulation; KPI, Key Performance Indicator; UHI, Urban Heat Island; LHS, Latin Hypercube Sampling; RCP, Representative Concentration Pathways; TMY, Typical Meteorological Year; TDY, Typical Downscaled Year; ECY, Extreme Cold Year; EWY, Extreme Warm Year; HDD, Heating degree Day; CDD, Cooling Degree Day; GCM, Global Climate Model; RCM, Regional Climate Model; F-TMY, Future Typical Meteorological Year; EPW, EnergyPlus Weather file; SRC, Standardized Regression Coefficients; CCOR, Climate Change Overheating Resistivity; IohD, Indoor overheating Degree; MBE, Mean Bias Error; CVRMSE, Coefficient of Variation of Root Mean Squared Error.

* Corresponding author.
E-mail addresses: Milad.heiranipour@polito.it (M. Heiranipour), Miren.juaristigutierrez@eurac.edu (M. Juaristi), Stefano.avesani@eurac.edu (S. Avesani), Fabio.favoino@polito.it (F. Favoino).

https://doi.org/10.1016/j.buildenv.2025.113459
Received 31 January 2025; Received in revised form 10 June 2025; Accepted 18 July 2025
Available online 23 July 2025

Nomenclature

Symbols

α	Solar absorptance[-]
λ	Thermal conductivity [W/mK]
σ_m	Monthly variance
$\Delta\bar{X}_m$	Absolute monthly change in climate variable
P_h	Stochastic parameter for hourly data generation

Variables

ACH	Air changes per hour [h^{-1}]
COP	Coefficient of Performance [-]
SEER	Seasonal Energy Efficiency Ratio [-]
EUI	Energy Use Intensity [kWh/m^2]
IohD	Indoor overheating Degree [°C]
g-value	Solar heat gain coefficient [-]
U-value	Thermal transmittance [W/m^2K]
Y-value	Periodic thermal transmittance [W/m^2K]
Sf	Sobol First Index [-]
St	Sobol Total Index [-]
SRC	Standardized Regression Coefficients [-]
Tmin	Minimum temperature setpoint [°C]
Tmax	Maximum temperature setpoint [°C]
Tdaily	Daily average temperature [°C]

1. Introduction

Climate change, characterized by a global average temperature increase of approximately 1.1 °C above pre-industrial levels, poses significant challenges to energy consumption, economies, and public health. The IPCC Sixth Assessment Report highlights that climate impacts are occurring more rapidly, with greater intensity, and are more widespread than previously anticipated [1]. Buildings are particularly vulnerable to these changing conditions, as increased climate variability and extreme weather events, especially heatwaves, impact human well-being, thermal comfort, and energy demand [2–4]. Studies show that heat disproportionately affects vulnerable groups [5–8], including the elderly [9], children [10], people with pre-existing health conditions [11–13], and socio-economically disadvantaged communities [14,15]. Research demonstrates that people with occupational heat exposure are up to five times more likely to die during extreme heat events [16,17]. These populations often have limited access to cooling resources and face higher mortality risks during extreme heat events [18,19], highlighting the urgent need for heat-resilient building solutions that can maintain acceptable indoor conditions despite changing outdoor environments.

For these reasons, assessing and improving the adaptive capacity of buildings has become increasingly critical [20], with particular attention being paid to facade design decisions that can enhance building thermal resilience related to climate change impacts. Thermal resilience of buildings refers to their capacity to maintain a comfortable indoor environment under future climate scenarios(typical and extreme condition) [21,22]. Key factors influencing thermal resilience include outdoor climate conditions, building characteristics (such as envelope design and HVAC systems), occupant behaviours, and the reliability of the local power grid [22]. While Building Performance Simulation (BPS) has traditionally been used to assess annual energy consumption using historical climate data, it is increasingly being used to analyses thermal resilience under future climate scenarios [23]. However, the reliability and accuracy of these assessments is heavily dependent on the future weather data used (as boundary condition), which can have a significant impact on the evaluation of different design strategies [24].

These boundary conditions are defined by climate projections based on various greenhouse gas emission scenarios, known as Representative Concentration Pathways (RCPs) [25], which introduce significant uncertainties in defining boundary conditions for climate-resilient building design [26]. These uncertainties are further compounded by the absence of standardized metrics and methodologies for evaluating methods [27], making it challenging to consistently assess building performance across different studies. The generation of future weather files for BPS requires the processing of these climate projections using various models and methodologies [28] which are primarily based on scenarios outlined in IPCC reports [25] and embedded in Global Climate Models (GCMs) available through open-source databases [29]. This data requires further processing to be useful for BPS. Specifically, GCM data must undergo downscaling to create location-specific future weather data suitable for building simulation, which can be accomplished through two main approaches: statistical and dynamical methods [30].

Dynamical downscaling employs Regional Climate Models (RCMs) nested within GCMs [31], to provide fine-scale climate data by simulating atmospheric and land processes. This physical-based process using Regional Climate Models (RCMs) nested within Global Circulation Models (GCMs), producing physically coherent datasets with higher temporal and spatial resolution [32–34]. While this method demands considerable computational resources, it offers high-resolution results, as demonstrated by tools like the Rossby Centre Regional Atmospheric Climate Model (RCA4) [35], which provides detailed climate projections for specific regions [29]. This method has been demonstrated to excel at representing extreme weather events, local climate features, and topographical influences without being constrained by historical observations [36,28]. It is particularly suitable for studies requiring detailed representation of complex regional climate phenomena, urban heat island effects, and future weather extremes. This approach is especially valuable for localized impact studies and scenarios where capturing temporal detail and extremes is critical [37], as demonstrated by Nik [38] who synthesized Typical Downscaled Year (TDY), Extreme Cold Year (ECY), and Extreme Warm Year (EWY) scenarios from RCM data.

In contrast, statistical downscaling offers a more computationally efficient alternative by estimating regional conditions from larger-scale climate data. Statistical downscaling can be categorized into two main approaches: morphing and stochastic methods. The morphing (implemented in CCWeatherGen) [39] is a popular statistical technique, has been demonstrated to successfully produce future weather files for Heating Degree Day (HDD), Cooling Degree Day (CDD) calculations. Furthermore, it has been shown to exhibit a high degree of agreement with raw climate model outputs [36]. However, it inherently preserves the characteristics of current weather data, thereby failing to capture fluctuations across seasonal to hourly scales and underrepresenting extreme events, such as heat waves [36,32,38]. The stochastic method (implemented in Meteonorm) approaches [40], leverages dominant variables (e.g., solar radiation) and local statistical data to synthesize high-resolution typical years, yet it faces challenges in accurately modelling a broad range of climatic variables, which can lead to inconsistencies in the generated weather series [41]. While statistical methods offer computational efficiency and ease of use—ideal for large-scale or preliminary studies—they typically provide lower temporal precision than dynamical downscaling.

Both dynamical and statistical downscaling approaches rely on GCM inputs and use multiple climate model simulations with varying initial conditions to better represent the range of possible future climate scenarios. This ensemble approach helps capture the inherent uncertainties in climate projection [42]. The choice between these methods typically depends on project-specific requirements, available computational resources, and desired level of accuracy [43]. Recent research has shown that different downscaling approaches used to generate future weather files can lead to variations of up to 18 % in predicted thermal performance metrics [24,44,37,45]. This variability in weather file generation methods raises important questions about how such methodological differences might influence on facade design decisions [46].

In fact, building envelopes play a crucial role in mediating between indoor and outdoor environments, significantly influencing both occupant comfort and building energy performance [47] and thus, thermal resilience of buildings. Prior research has extensively examined the relationship between façade design strategies and building thermal resilience under changing climate conditions, employing diverse methodological approaches across various climate zones. These studies have investigated different aspects of envelope performance, from basic thermal properties to complex dynamic behaviours. For instance, studies like Tettey et al. [48] have analysed multi-story buildings using statistical downscaling methods, finding that parameters such as orientation, Window-to-Wall Ratio (WWR), and glazing properties significantly influence energy performance under future climate scenarios. Similarly, Karimpour et al. [49] employed dynamical downscaling to evaluate envelope design in Mediterranean climates, revealing that by 2070, building design priorities will shift from balanced heating-cooling to predominantly cooling concerns. Zhang et al. [50] conducted a comprehensive assessment using both statistical and dynamical methods, emphasizing the importance of combining multiple cooling strategies in early design phases. These studies demonstrate that while façade parameters consistently impact building performance, their relative importance varies depending on climate context and assessment methodology.

The methodological approaches to future climate assessment in these studies reveal important patterns and limitations in current research. While some researchers such as Krelling et al. [51] and Ji et al. [52] utilized sophisticated dynamical downscaling methods to generate future weather data, others opted for more accessible statistical approaches due to computational constraints. These different methodological approaches raise questions about the comparative reliability of different downscaling techniques for façade design optimization. Notably, most studies focus on either statistical or dynamical methods exclusively, with few comparing their relative impacts on design decisions. For instance, Amaripadath et al. [53] and Passer et al. [54] demonstrated that high-quality envelope retrofits could significantly improve building resilience, but their conclusions were based on single downscaling methods. Additionally, while studies like Sehizadeh and Ge [55] identified potential risks in high-performance standards like PassivHaus under future climates, the influence of weather file generation methods on these findings remains unclear. Table 1 presents several key publications that explore the impact of façade design strategies on thermal resilience in the context of climate change.

A key challenge lies in the generation and application of future weather data for BPS. While studies have demonstrated variations in building performance predictions using different weather datasets [30, 37] two critical limitations remain inadequately addressed in current research. Firstly, the impact of façade design strategies on building performance remains an area of research that has not yet been fully explored, particularly in relation to the evaluation of typical long-term weather conditions. These conditions are instrumental in informing fundamental design choices at the early stage of a project. Secondly, most existing studies (as reported in Table 1) focus on individual performance aspects, such as energy use, thermal comfort, or environmental impact separately (even though multiple performance metrics are used for that specific single aspect), rather than providing a comprehensive assessment of how façade strategies influence multiple dimensions of building thermal resilience. As Duan et al. [61] have highlighted, this siloed approach fails to capture important trade-offs between different performance objectives and obscures how various downscaling methods might differently affect these relationships both in absolute and comparative terms. This fragmented understanding is becoming increasingly critical as buildings face multiple, often competing, performance demands under changing climate conditions that require integrated solutions addressing energy efficiency, occupant wellbeing, and environmental impact simultaneously.

This study aims to address a central research question: *How do different methodologies for generating typical future weather files influence early-stage façade decision*-making *aimed at improving thermal resilience?* To comprehensively examine this question, three specific aspects are explored:

1. What does it mean designing facades for building thermal resilience in practice and which Key Performance Indicators (KPIs) effectively define thermal resilience objectives?
2. How do different future weather file methodologies compare in terms of their absolute impact on façade design performance, specifically relating to thermal resilience KPIs?
3. How these different weather file methodologies influence the comparative analysis between façade design strategies in early-stage design, particularly focusing on how they affect the ranking of design options from different KPI perspectives?

To address these questions the paper is structured in the following way: (i) in the methodology section a framework for evaluating thermal resilience is firstly establish through specific KPIs including energy performance, indoor discomfort, and heat release from building to the urban environment, (ii) different downscaling methods for generating future typical meteorological year (F-TMY) data are analysed and compared; (iii) then the methodological framework is provided to perform absolute and comparative performance-based evaluations of façade design strategies, by means of global sensitivity analysis methodologies; (iv) finally a description of the specific case study and façade design strategies under analysis is provided. In the result section, the results from the sensitivity analysis are discussed in absolute and comparative terms, according to each specific building heat resilience KPI, and finally discussing all the main KPIs together. This approach allows us to understand not only the practical implications of different weather file generation methods but also their influence on early-stage façade design decisions on final impact related to building heat resilience, as well as façade design strategies that could favour heat resilience in a more comprehensive way, rather than focusing on a single performance aspect only.

2. Methodology

As illustrated in the methodology diagram in Fig. 1, this study presents a comprehensive approach that evaluates how different weather file generation methods influence façade design decisions for climate-resilient buildings. The first step consists in the definition of outdoor boundary conditions, that is, the generation of future weather datasets through both dynamical downscaling using Regional Climate Models (RCM) and statistical methods including morphing and stochastic approaches. These weather files establish the climatic boundary conditions for subsequent analyses.

The methodology then focuses on defining façade design parameters and their ranges of variation. Four key aspects are examined: (1) insulating capability of both opaque and transparent envelope components, (2) total solar transmission through fenestration systems (incorporating window characteristics and shading devices), (3) solar absorption of opaque surfaces, and (4) ventilative heat transfer mechanisms via either natural or mechanical means. To isolate the effects of building envelope design choices, these parameters are incorporated into a room-based energy model using the standardized BESTEST case 600 configuration. This approach allows for controlled comparison of façade performance variables without the confounding influence of complex building geometries or systems. Computational efficiency is optimized through Latin Hypercube Sampling (LHS), which enables systematic parameter space exploration while minimizing simulation runs. This sampling strategy ensures comprehensive coverage of possible design configurations across multiple future climate scenarios.

The resulting simulation data undergoes both absolute value analysis and global sensitivity assessment to evaluate façade design effectiveness

Table 1
Summary of articles evaluating thermal resilience of building façade strategies under climate change.

Ref	Climate (Köppen)	Type of Weather Data					Key Performance Indicators(KPIs)	Facade/Design Strategies	Significant Findings
		Type of downscaling		Time scale					
		Statistical	Dynamical	H	M	F			
[48]	Dfb	*			*	*	EUI, effectiveness of design strategies	Orientation, WWR, U-value and g-value of window, solar shading, ventilation rate,	Overall, annual total operation primary energy decreased by 37–54 % for the building versions when all strategies are implemented under the considered climate scenarios.
[50]	Various	*	*	*	*	*	EUI, Absorptive, adaptive, restorative capacity, recovery speed, thermal comfort and resilience	advanced solar shading, cool envelope materials, green roofs, ventilated facades, thermal mass utilization, ventilative cooling, evaporative cooling, compression refrigeration, absorption refrigeration, ground source cooling, sky radiative cooling	For resilient cooling in buildings, combining multiple cooling strategies with different capacities must be considered in the early design phase, to improve resilience against climate change.
[56]	Cfa		*	*			SET, HI, Hours of Safety, EUI, backup power capacity	Passive envelope measures (insulation of exterior walls and roofs, cool coatings for walls and roofs, interior window shades, solar window film, building envelope sealing, natural ventilation),	While a passive building envelope improves thermal resilience, implementing energy efficiency measures can lower the needed backup power capacity by 19 %.
[49]	Csa		*		*		EUI, Peak load, star rating (energy efficiency)	External wall insulation, internal wall insulation, roof insulation, reflective foil, thermally reflective roofs, different floor coverings	By 2070, climate change will shift building design priorities from balancing heating and cooling to predominantly focusing on cooling.
[54]	Cfb		*	*	*	*	EUI(non-renewable), GWP, surplus electricity production, energy payback time.	Minimum and high-quality façade refurbishment, prefabricated façade elements, solar thermal collectors, photovoltaic (PV) panels	High-quality building refurbishment utilizing prefabricated façade elements integrated with solar collectors and PV offers an optimal renovation strategy from an LCA perspective.
[51]	Cfa		*	*	*	*	TA, IohD, EUI, TV, Max T, tR	Passive strategies including cool roofs, cool walls, advanced glazing, solar shading, roof insulation, wall insulation, increased window openable area, and pre-cooling	The study revealed that median cooling energy consumption could rise by 48 % by the 2050s without the implementation of resilience strategies.
[55]	Dfb	*		*	*	*	IohD, peak load, EUI	Retrofitting to PassiveHaus standard including high insulation, airtight envelope, passive solar gain, heat recovery, daylighting, shading, energy-efficient appliances, and high-performing windows	High-performance building standards like PassivHaus achieve significant energy savings but must carefully balance this against increased overheating risks under future climate scenarios.
[57]	Csa and Cfa		*	*			OHL, thermal habitability, thermal tolerability	WWR, window glazing type, exterior wall insulation, wall reflectance, roof insulation, roof reflectance, occupant density, plug load density, and orientation	This study determined that OHL may be used as a key resilience metric for assessing how prepared an office building will be when faced with the possibility of a power outage.
[53]	Csa		*	*			Indoor temperature, EUI, peak load, IohD	High thermal mass, external shading devices, night ventilation, and passive cooling strategies	Existing building-level renovation strategies alone are insufficient to prevent overheating in renovated dwellings and will require the addition of active cooling systems.
[52]	Dfb		*	*	*	*	TRI, SET, IohD, EUI	Various passive cooling retrofits including cool roofs, advanced glazing, natural ventilation, and increased insulation	The researchers developed and validated a Thermal Resilience Index and labelling system to quantify building thermal resilience, showing that retrofit combinations can enhance resilience by 50–70 % compared to baseline conditions.
[58]	Dfb		*	*	*	*	Surface temperature, R-value, dynamic thermal transmittance, moisture content,	Wood stud wall with cavity insulation and exterior insulation (XPS and mineral wool), pre-cast concrete cladding, air barrier, OSB sheathing, gypsum board	The findings demonstrate façade thermal performance varies significantly under different climate scenarios, with TMY weather data overestimating performance compared to hourly analysis.
[24]	Csa	*		*	*	*	Indoor and outdoor surface temperature, EUI, thermal transmittance	Brick facade with double-glazed windows (test cell) and single-glazed windows (multi-family building), exterior walls with specific U-values for insulation analysis	Results revealed that future weather data projection methods significantly affect building thermal performance predictions, with up to 18 % variation in summer discomfort hours and 12 kWh/m2 difference in cooling demand between methods.
[59]	Cfb	*		*			IohD, HE, WBGT, HI	Thermal transmittance, Thermal mass, WWR	The proposed multi-criteria certification scheme successfully evaluated building thermal resilience

(*continued on next page*)

Table 1 (*continued*)

Ref	Climate (Köppen)	Type of Weather Data					Key Performance Indicators(KPIs)	Facade/Design Strategies	Significant Findings
		Type of downscaling		Time scale					
		Statistical	Dynamical	H	M	F			
									across IOD, HE, WBGT, and HI metrics, providing a standardized framework for assessing and improving building performance under extreme heat conditions.
[60]	Mix	*		*	*	*	TWEH26, OT	Thermal mass, Shading, Pitched roof with dormers	Regional and urban climate conditions significantly impact indoor thermal performance, necessitating location-specific assessments in building design, with night-time temperatures playing a crucial role in heat accumulation.

H: Historical, M: Mid future, F:Future, EUI: Energy Use Intensity, IohD: Indoor overheating Degree, OHL: Occupancy Hours Lost, HI: Heat Index, GWP: Global Warming Potential, TA: Thermal Autonomy, TV: Thermal Vulnerability, Max T: Maximum indoor air Temperature, tR: time Recovery, SET: Standard Effective Temperature. TRI: Thermal Resilience Index, HE: Hours of exceedance, WBGT: Wet-bulb globe temperature, TWEH26: Temperature-weighted exceedance hours above 26 °C, OT: Operational Temperature.

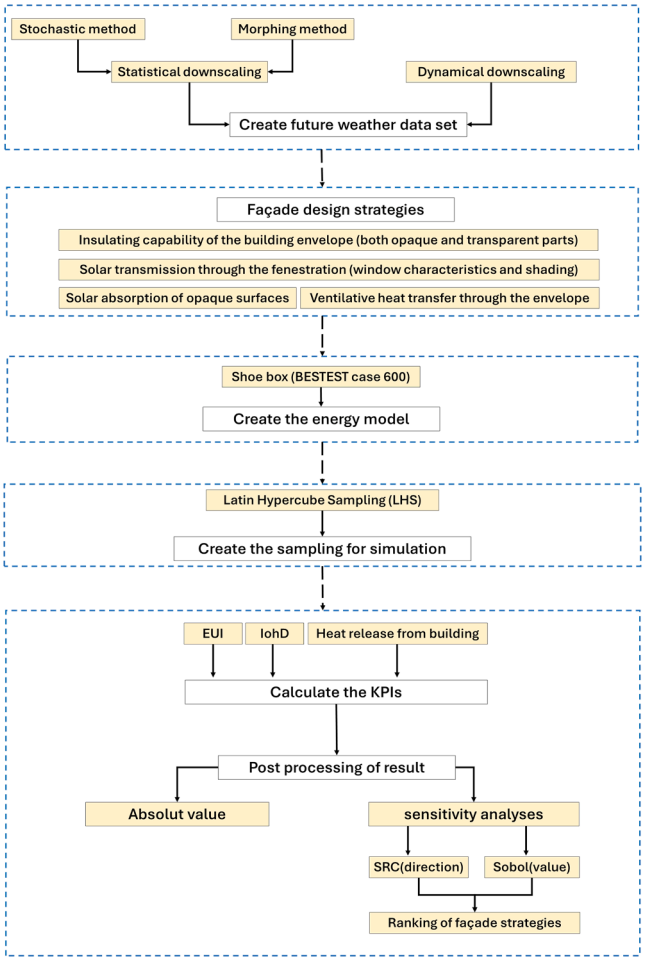

Fig. 1. Methodological steps.

according to three primary thermal resilience objectives: energy performance optimization, indoor thermal comfort enhancement, and reduction of heat release from buildings to the urban environment. This multifaceted assessment framework is applied across three-time horizons (2020, 2050, and 2080) to understand the evolving importance of various façade strategies under changing climatic conditions.

2.1. Definition of the outdoor climatic boundary condition

For this study, Turin, Italy was chosen as a representative European temperate climate, classified as Cfa (humid subtropical) in the Köppen climate classification. The selection of Turin as case study location was based on several critical considerations. First, its temperate climate presents a balanced heating and cooling demand profile in the current climate, allowing for comprehensive assessment of façade design strategies under both thermal conditions. This balance is crucial for understanding the full range of resilience measures rather than focusing exclusively on cooling-dominated or heating-dominated climates. Secondly, Turin's location in the Po Valley positions it as a climate change 'hotspot' within Europe. The region is projected to face significant climate-related challenges, including higher temperatures, more intense heat waves, and altered precipitation patterns, making it particularly vulnerable to climate change impacts [62–64]. This heightened vulnerability makes Turin an ideal location for examining building adaptation strategies. Third, the availability of comprehensive meteorological data was a key selection factor. Turin benefits from 15 years of continuous hourly meteorological observations provided by the Regional Agency for Environmental Protection of Piedmont (ARPA Piemonte) [65,66], including air temperature, relative humidity, wind speed and direction, and global solar radiation. This extensive dataset exceeds the minimum requirement of 5 years of observational data necessary for bias adjustment in dynamical downscaling procedures, enabling thorough technical validation of the generated weather files.

The analysis examines three temporal horizons: current (2020), mid-future (2050), and future (2080), adopting climate projections based on RCP 8.5. This scenario was chosen as it represents a high-emission trajectory, often referred to as a 'business-as-usual' pathway, reflecting limited climate mitigation efforts [28]. The IPCC AR6 highlights RCP 8.5′s utility in assessing the upper bounds of climate risks, making it particularly important in building performance simulations (BPS). It provides a worst-case benchmark, ensuring that façade designs are resilient under the most extreme climate projections [67]. RCP 8.5 can serve as a useful reference point for the assessment of near-term climate risk, as suggested by some studies which indicate that historical cumulative CO2 emissions between 2005–2020 have closely aligned with RCP 8.5 projections [68]. This potential correspondence with observed emission trends may render RCP 8.5 suitable for the evaluation of building performance scenarios through mid-century. Notwithstanding the ongoing discourse among researchers regarding its plausibility as a long-term trajectory, RCP 8.5 could help capture certain carbon-cycle feedback that might be less represented in lower-emission scenarios [61].

The methodology encompasses both dynamical and statistical

downscaling approaches. The dynamical downscaling method implemented by the IEA EBC Annex 80 group [69] generates typical and extreme weather files with particular attention to heat wave conditions. Statistical downscaling is performed using two established tools: CCWeatherGen [70] and Meteonorm [40]. CCWeatherGen uses a morphing-based statistical method to adjust historical weather data by incorporating changes predicted by global climate models to produce future weather files. This approach modifies key climate parameters such as temperature, solar radiation and precipitation while preserving the temporal structure of the original dataset. It is computationally efficient and is often used for scenarios that require rapid and scalable analysis. Meteonorm, on the other hand, uses a stochastic weather generation method that combines interpolation of measured historical data with statistical synthesis to generate future weather files. This method considers typical weather conditions and provides location-specific and detailed outputs. While CCWeatherGen is advantageous for its simplicity and speed, Meteonorm provides more nuanced data sets, suitable for applications requiring greater precision and customisation based on local climatic inputs [30].

Dynamical downscaling begins with raw outputs from General Circulation Models (GCMs), which provide large-scale climate data at a coarse spatial resolution. These outputs are then refined through Regional Climate Models (RCMs), which incorporate regional topographic and climatic features and vegetation. This step enhances the resolution and accuracy of localized projections. Following this, bias correction is applied to adjust the RCM outputs using long-term observational datasets, ensuring alignment with historical climate conditions. Advanced methods such as Quantile Delta Mapping (QDM) and Multivariate Bias Correction (MBCn) are employed to correct biases across multiple climate variables while preserving their interdependencies. Finally, the corrected datasets are processed to generate weather files in formats suitable for building performance simulations, including both typical meteorological years (TMYs) and extreme weather scenarios, such as heatwave years (HWYs). This comprehensive approach ensures that the weather files are both accurate and reliable for assessing the resilience of buildings under future climate conditions [69]. The complete process of weather dataset generation is illustrated in Fig. 2. Table 2 summarizes the generated weather files sets for the selected location.

The study employs a range of statistical techniques to assess the accuracy of the weather data, comparing the climate projection of current scenario (2006 to 2020) with observations from same period. The primary statistical indicators employed are the Mean Bias Error (MBE) and the Coefficient of Variation of Root Mean Squared Error (CVRMSE), in accordance with the guidelines set forth by ASHRAE [72]. In the case of these metrics, the maximum threshold for hourly calibrated data is set at 10 % for MBE and 30 % for CVRMSE, in accordance with the guidelines set forth in reference [72]. Furthermore, the evaluation incorporates the *d*-index (index of agreement) [73], along with probability density functions (PDF) and cumulative distribution functions (CDF), which are employed to assess the statistical distributions of the weather parameters [74]. This statistical analysis compares multiyear raw climate outputs and bias-adjusted datasets with observational data for Turin, examining air temperature, relative humidity, global solar irradiance, and wind speed during the current period. The combination of multiple statistical indicators and distribution analyses ensures a thorough evaluation of different weather file generation methods and their accuracy in representing both current and future climate conditions for BPS.

2.2. Building model and façade design strategies

2.2.1. Building model and characteristics

In order to assess the impact of early-stage façade design decision, a simplified single-zone virtual model is adopted [75–77] using the BESTest 600 ASHRAE Standard 140–2017 [78,79] (Fig. 3). The analysis focuses on a South-oriented office space, deliberately chosen to isolate and examine the impact of different weather file generation methods on façade early-stage design decisions. This simplified approach enables a focused investigation of building envelope parameters without the added complexity of inter-zone interactions or multiple orientations. While this approach allows for clear identification of parameter sensitivities without the confounding influence of inter-zone interactions, it has several important limitations that must be acknowledged. First, the model cannot capture the complexities of multi-zone HVAC operations, including load diversity and system interactions that would occur in actual buildings. Second, it does not account for variations in occupant behaviour and internal load profiles across different spaces, which can significantly influence both energy use and thermal comfort. Third, by focusing exclusively on south orientation, the model does not represent solar gain heterogeneity and differential façade performance across various orientations that would characterize a complete building envelope. While this methodological choice limits the generalizability of specific façade strategy recommendations, it provides a clear framework for understanding how different weather data generation methods could influence building envelope related design decisions.

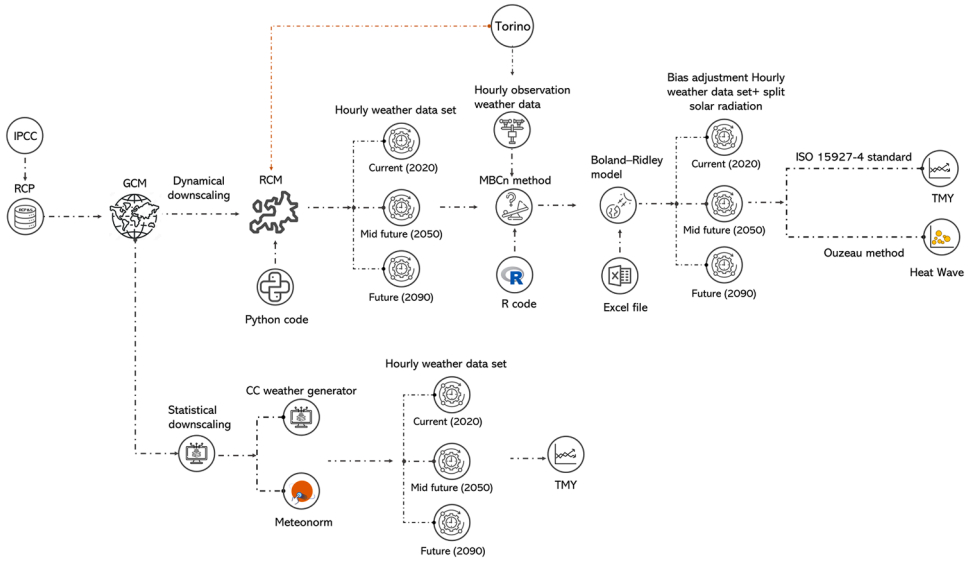

Fig. 2. Process of current and future weather data set.

Table 2
Future weather datasets (Turin) [71].

No	Type of downscaling	method	Type of data	Year	Code
1	Statistical(Morhing)	CCWeatherGen	TMY	Current	St_CC_TMY_2020_Ex_8.5
2	Statistical(Morhing)	CCWeatherGen	TMY	Mid future	St_CC_TMY_2050_Ex_8.5
3	Statistical(Morhing)	CCWeatherGen	TMY	Future	St_CC_TMY_2080_Ex_8.5
4	Statistical(stochastic)	Meteonorm	TMY	Current	St_Meto_TMY_2020_Ex_8.5
5	Statistical(stochastic)	Meteonorm	TMY	Mid future	St_Meto_TMY_2050_Ex_8.5
6	Statistical(stochastic)	Meteonorm	TMY	Future	St_Meto_TMY_2080_Ex_8.5
7	Dynamical	RCM	TMY	Current	Dy_RCM_TMY_2020_Ex_8.5
8	Dynamical	RCM	TMY	Mid future	Dy_RCM_TMY_2050_Ex_8.5
9	Dynamical	RCM	TMY	Future	Dy_RCM_TMY_2080_Ex_8.5

TMY = Typical Meteorological Year.

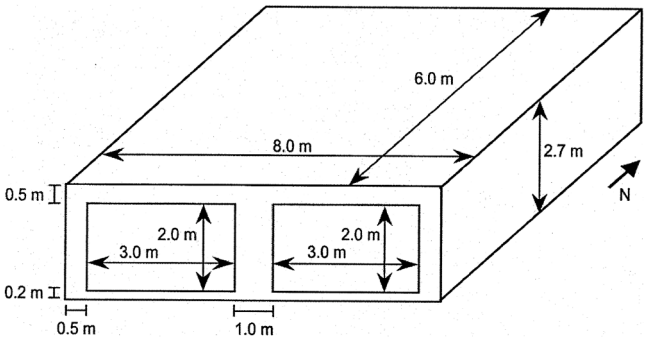

Fig. 3. Sun-oriented office reference room geometry - BESTest No.600 [78].

The room model incorporates detailed specifications for wall construction, insulation, window types, HVAC systems, and internal schedules and loads as outlined in Table 3. In this study, lighting energy consumption is calculated using a continuous dimming method designed to maintain a threshold illuminance of 300 lx in the reference point, in the centre of the room. Illuminance calculations are performed using Delight EnergyPlus module, incorporating split flux methods for daylight analysis.

Table 3
Design parameters used as simulation inputs for modelling.

	Values	Ref
Geometrical parameter		
Total area (m^2)	48	[78]
Total volume (m^3)	129.6	[78]
Shading depth	[Parametric]	
Internal heat gains		
No. of occupants	4	[78]
Occupancy schedule	Office	[80]
Metabolic rate (Met)	1.2 (Sedentary work)	[81]
Lighting density (W/m^2)	7	[82]
Lighting schedule	Office, continuous dimming	[80]
Equipment load (W/m^2)	3.125	[51]
Equipment schedule	Office	[80]
Thermal characteristics		
Ground floor thermal transmittance (W/m^2K)	Adiabatic	
External roof thermal transmittance (W/m^2K)	Adiabatic	
Nort, East, West wall thermal transmittance (W/m^2K)	Adiabatic	
Wall thermal transmittance (W/m^2K)	[Parametric]	
Window thermal transmittance (W/m^2K)	[Parametric]	
Infiltration and ventilation parameters		
Infiltration rate (m^3/s per m^2 facade)	0.005	[79]
Mechanical ventilation rate (m^3/s per m^2 area)	[Parametric]	
Operable area for natural ventilation (m^2)	4 (2 m^2 per each window)	
Setpoint for natural ventilation (°C)	[Parametric]	
HVAC characteristics		
Heating setpoint (°C)	20	[78]
Cooling setpoint (°C)	26	[45]
HVAC system	Ideal air load	
Coefficient of Performance (COP) - Seasonal Energy Efficiency Ratio (SEER)	2.5–3.5	[83]
HVAC schedule	Office	[80]

2.2.2. *Façade design strategies*

The analysis examines four key building envelope characteristics and their associated design parameters:

- **Heat Transfer Performance (Opaque and transparent)**

The opaque envelope consists of a multi-layer wall construction: interior finishing, brick wall, expanded polystyrene (EPS) insulation layer (λ = 0.035 W/mK) of variable thickness, and exterior finishing (Fig. 4). The thermal transmittance (U-value) of this assembly varies based on the insulation thickness are:

- No insulation (U-value = 2.36 W/m^2K, Y-value = 1.506 W/m^2K);
- 5 cm (U-value = 0.63 W/m^2K, Y-value = 0.169 W/m^2K);
- 15 cm (U-value = 0.26 W/m^2K, Y-value = 0.057 W/m^2K);
- 25 cm (U-value = 0.16 W/m^2K, Y-value = 0.027 W/m^2K).

For transparent components, two glazing configurations are evaluated: double and triple glazing systems. The double-glazing units (U = 1.36 W/m^2K) consist of Wood frames with 16 mm 90 % Argon-filled cavity. The triple glazing system (U = 0.97 W/m^2K) employs Insulated Fiberglass/Vinyl frames, also with 16 mm 90 % Argon-filled cavity. In the case of the opaque envelope components, three different exterior finishing colours are evaluated based on their solar absorptance (α) values.

- White (α = 0.35), high solar reflectance and minimal heat absorption,
- light grey (α = 0.55), moderate solar radiation absorption,

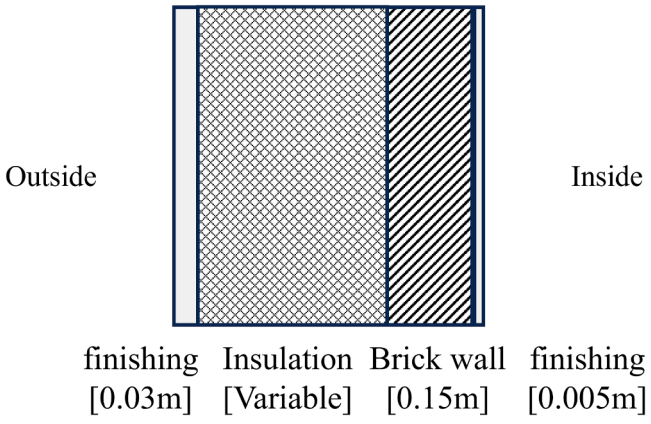

Fig. 4. Wall construction section.

- Dark grey (α = 0.85),high solar absorption.

- **Solar Heat Gain Control**

The amount of Solar heat gain through the transparent envelope is varied in the parametric simulation by means of either: (i) varying the window-to-wall ratio (WWR) from a minimum of 40 % to a maximum of 75 %, with an intermediate value of 55 %, directly influencing the proportion of glazed surface area available for solar transmission; (ii) the presence of a horizontal overhang positioned immediately above the windows, with depths ranging from no shading to 100 cm (in steps of 20 cm); (iii) the glazing specifications combining different coatings (low-E or selective) to achieve varying levels of visible light transmission (0.70 and 0.40) and solar heat gain coefficients (0.55, 0.35, and 0.20).

- **Ventilation Configuration**

Ventilation control strategies encompass both mechanical and natural ventilation systems. The mechanical ventilation system operates at three different air change rates: a baseline rate of 1.88 ACH (corresponding to the minimum ventilation requirement for Category II buildings according to EN ISO 16,798 [84]), a moderate rate of 3.76 ACH, and an enhanced rate of 5.63 ACH. Natural ventilation is controlled through an automated window operation system with a fixed operable area of 4 m^2 (2 m^2 per window) that follows a dual-criterion decision process. The primary control evaluates whether the outdoor air temperature falls within acceptable bounds (between T_{min} as a variable parameter and T_{max} fixed at 27 °C) for ventilation. If this condition is met and the zone is occupied with an indoor air temperature exceeding 25 °C, the windows open to provide immediate cooling. The secondary control utilizes daily average temperature (T_{daily}) to enable night cooling. When T_{daily} exceeds 18 °C, windows can open during unoccupied periods to reduce overheating through night ventilation. The windows automatically close if any of these conditions are not satisfied, ensuring effective free cooling while maintaining occupant comfort and preventing overcooling. The complete control logic for window operation is illustrated in the flow diagram in Fig. 5, which shows the sequential decision process and the interaction between temperature conditions and occupancy schedules.

Table 4 summarizes all design parameters, with a reference building envelope configuration representing values that meet the minimum requirements of the Italian building energy code DM 26/06/2015 [85]. The reference building values include 55 % WWR, double selective glazing (70_35), 15 cm insulation thickness, light grey finishing, and minimum ventilation rate for Category II buildings.

2.3. Simulation analysis process

A simulation workflow using BPS was implemented to assess the building's performance and thermal resilience of the building. The initial model was developed using the parametric capabilities of Grasshopper 1.0.0007 within Rhino 7 (SR31). Subsequent analyses were performed using Ladybug Tools 1.8.0 [86], which integrates EnergyPlus and OpenStudio for thermal calculations [87,65] Given the extensive number of possible variable combinations in a full factorial analysis (resulting in 93,312 simulations), Latin Hypercube Sampling (LHS) [88] was adopted to optimize computational efficiency while maintaining statistical robustness. Parameter boundaries were set to capture realistic design options while ensuring exploration of both conventional and progressive design strategies. To determine the appropriate sample size, a convergence analysis was conducted through preliminary sensitivity trials with 10, 20, 50, and 100 sets of inputs. These trials demonstrated that 50 sets of inputs (generating 1300 sample points) provided an optimal balance between computational efficiency and statistical robustness. At this sample size, the sensitivity indices stabilized with variations of less than 1 % when compared to larger samples, indicating sufficient convergence. This sampling approach ensured comprehensive coverage of the parameter space while maintaining computational feasibility across all nine weather scenarios. This sampling approach resulted in a total of 11,700 simulations across all scenarios while ensuring reliable coverage of the parameter space.

The simulation workflow consists of three main phases: (1) parameter definition, where simulation parameters and future weather scenarios (F-TMY) are established, (2) model development, including the creation of parametric building and façade configurations, and (3) performance analysis using EnergyPlus for thermal calculations (Fig. 6). The entire process was automated using Python within the Grasshopper environment to streamline the analysis of multiple design scenarios.

2.4. Building thermal resilience Key Performance Indicators

The proposed framework aims to assess the thermal resilience of buildings according to three fundamental domains and scale: energy performance affecting the energy bills as well as operational carbon (further affecting a more regional / global scale), mitigation of the urban heat island effect (considering to urban scale), and indoor occupant discomfort (considering the local scale). These KPIs together could provide a more comprehensive assessment of a building's thermal resilience across multiple scales and impacts.

Energy KPIs focuses on maintaining or reducing energy use and heating/cooling loads as the climate changes, thereby minimizing CO_2 emissions from building operations. This is assessed by means of delivered Energy Use Intensity (EUI) and peak loads. EUI, measured in KWh/m^2, quantifies annual energy consumption for cooling, heating, lighting,

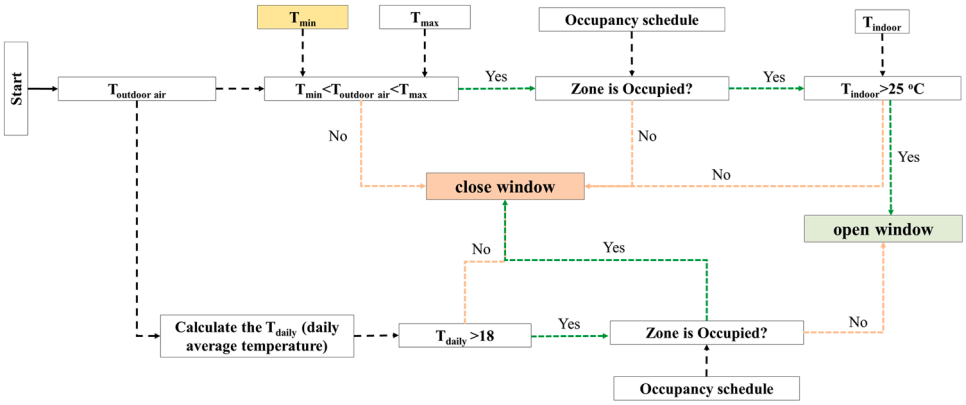

Fig. 5. control logic for window operation in natural ventilation.

Table 4
Facade design strategies.

WWR	Fenestration	Depth of shading	Depth of insulation	Colour of finishing	ventilation rate(m^3/s per m^2 area)	T_{min} for NV
55 %	Double_Selective_70_35 ($U = 1.36$)	without	15 cm($U = 0.26$) ($Y = 0.057$)	Ligh grey($\alpha = 0.55$)	0.0014(1.88 ACH)*	12 C
40 %	Double_LowE_70_55 ($U = 1.36$)	60 cm	Without($U = 2.36$) ($Y = 1.506$)	White($\alpha = 0.35$)	0.0028(3.76 ACH)	14 C
75 %	Double_selevtive_40_20 ($U = 1.36$)	80 cm	5cm($U = 0.63$) ($Y = 0.169$)	Dark grey($\alpha = 0.85$)	0.0042(5.63 ACH)	16 C
	Triple_Selective_70_35 ($U = 0.97$)	100 cm	25cm($U = 0.16$) ($Y = 0.027$)			
	Triple_LowE_70_55 ($U = 0.97$)					
	Triple_selevtive_40_20 ($U = 0.97$)					

α = solar absorptance, U = Heat transfer coefficient(W/m^2K),Y = Periodic thermal transmittance(W/m^2K), WWR = Window to wall Ratio, NV = Natural ventilation.
* corresponding to the minimum ventilation requirement for Category II buildings according to EN ISO 16798 [84].

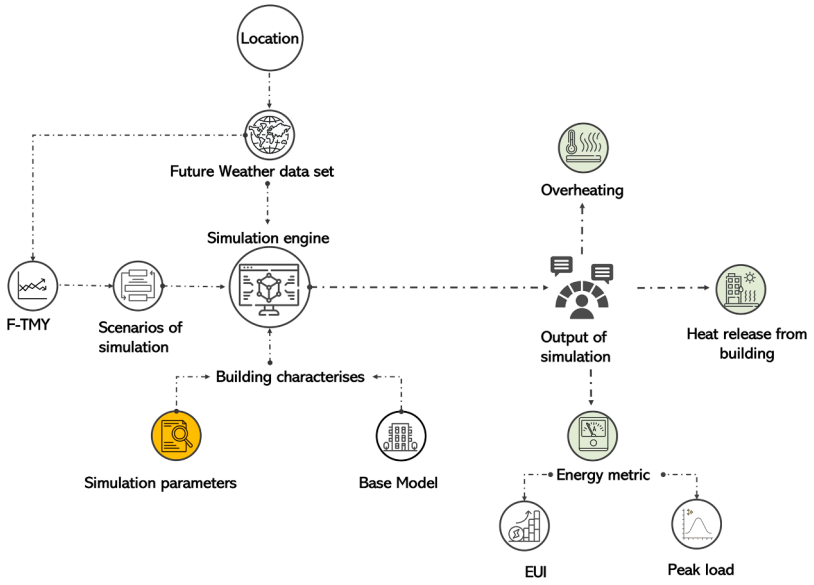

Fig. 6. simulation process.

and equipment. Delivered energy was specifically considered (instead of primary energy) to isolate building performance from grid considerations and primary energy factors, with calculations incorporating standard system efficiencies as defined in [89]. Peak load, measured in W/m^2 of floor area, evaluates the maximum heating and cooling demands, indicating the building's capacity to handle extreme energy requirements while maintaining functionality [51,90].

Indoor occupant discomfort is evaluated using the Indoor Overheating Degree (IohD), expressed in degrees Celsius (°C). This metric quantifies thermal discomfort over time and is linked to the robustness stage of resilience. By integrating time-based thermal discomfort data [51,91], IohD considers how effectively the building maintains comfortable conditions for occupants throughout the year.

Urban heat island mitigation is assessed through the building heat release, measured in kilowatt-hours per square meter of facade (kWh/m^2 facade). This metric quantifies the building's contribution to urban heating through three primary building sources: Air Conditioning (HVAC) systems, the exfiltration from the building zone, and the building envelope (both opaque and transparent components) [92].

2.5. Sensitivity analysis

In the present study two different sensitivity analysis methods are employed: (1) standardized regression analysis [93], a sampling-based method, and (2) Sobol's method [94], a variance-based method. Both methods provide quantitative measures of the sensitivity of the output variables to changes in input variables, allowing us to evaluate how different weather file generation approaches influence the perceived importance of various façade design parameters. Standardized regression analysis performs regression analyses on the input and output variables, eliminating the effects of different units by standardizing the variables by the ratio of the standard deviation to the mean. The resulting Standardized Regression Coefficients (SRCs) indicate the relative importance of each input variable. The sign (positive or negative) of an SRC indicates whether the input variable is positively or negatively correlated with the output variable. Sobol method determines the importance of input variables using a ratio of the input variable-related variance to the output variable variance. This method provides two key sensitivity indices: (i) Sobol First Index (Sf): accounts for the first-order effect of the input variable on the output variable; (ii) Sobol Total Index (St): Accounts for both the direct effect of the input variable and its interaction with other input variables. Both Sf and St are calculated using multi-dimensional Monte Carlo integration [95]. In this analysis, SRC was adopted for direct linear effects and Sobol total index for both direct and interaction effects. Considering both indicators provides a more holistic view of how different weather file generation methods impact the perceived importance of various façade design variables. By comparing the results across different weather file generation methods, it is possible to identify how the choice of method influences the sensitivity of façade design parameters, potentially leading to different design decisions for climate-resilient buildings [96].

To translate the sensitivity analysis results into actionable design recommendations, a systematic ranking approach was adopted that integrates SRC with Sobol total index. Initially, both positive and negative SRC values are extracted, which indicate whether a design parameter positively or negatively impacts KPIs such as IohD or EUI. Concurrently, the absolute values from the Sobol total index are obtained, which reflect each parameter's overall importance by accounting for linear and

non-linear effects as well as interactions with other design variables. The product of the Sobol total index with the sign of the related SRC is able to capture both the magnitude and the nature of each design parameter impact on the KPIs.

The subsequent ranking process involves ordering the design strategies based on the combined SRC and Sobol's total index values. Parameters with large negative values are identified as those where decreasing the parameter will lead to significant performance improvements, such as reducing energy consumption or mitigating overheating. Conversely, parameters with large positive values indicate that increasing the design parameter will decrease performance. This sorting creates a clear hierarchy of design strategies, ranging from the most critical adjustments needed to optimize specific performance indicators to the less critical ones. This hierarchical ranking enables designers to focus on the most influential parameters, ensuring that design decisions are both strategic and effective in enhancing building performance (Fig. 7).

To address the primary research question regarding the impact of different future weather file generation methods on façade design decisions, the ranking process is applied separately for each weather file generation method. By generating and comparing rankings from these diverse methods, for different future projections, consistent design recommendations can be identified that hold true across various weather file generation approaches.

3. Results

This section presents the main findings in two main parts. Firstly, the reliability of future weather data is assessed by comparing Future Typical Meteorological Year (F-TMY) files with observations for the current period. Then, the impact of different downscaling methods on building thermal resilience over three-time horizons (current, mid-future and future) is analyzed in two ways: (i) absolute differences between downscaling methods and (ii) comparative assessment of façade design strategies using sensitivity analysis, divided according to three main KPI areas identified to quantify building thermal resilience: energy performance, indoor thermal discomfort and urban heat island effect.

3.1. Reliability of downscaled weather datasets

To illustrate the distribution for the different weather scenarios, a box plot was created for the outdoor air temperatures trends for the current, mid-future, and future periods. This plot effectively displays the

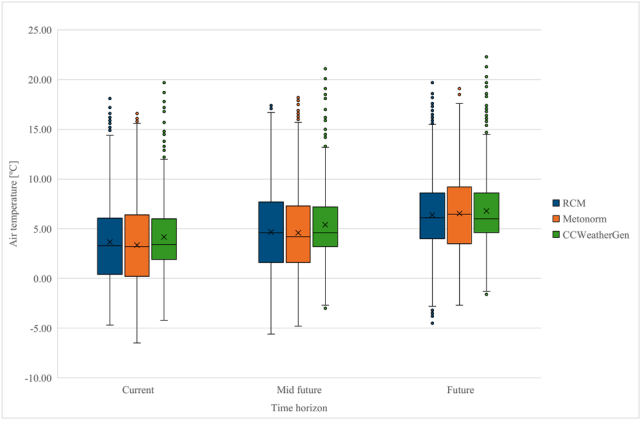

Fig. 8. Boxplot of air temperature values for each TMY EPW files.

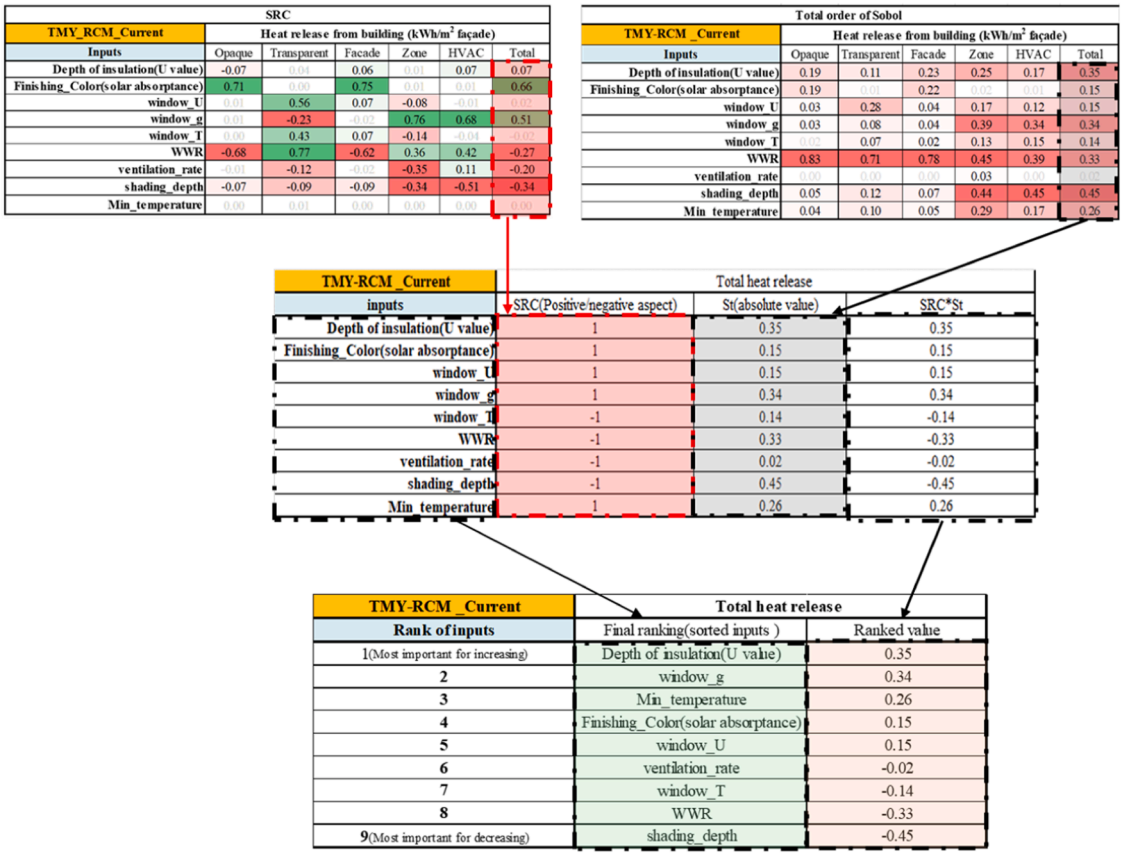

SRC

TMY_RCM_Current	Heat release from building (kWh/m² façade)					
Inputs	Opaque	Transparent	Facade	Zone	HVAC	Total
Depth of insulation(U value)	-0.07	0.04	0.06	0.01	0.07	0.07
Finishing_Color(solar absorptance)	0.71	0.00	0.75	0.01	0.01	0.66
window_U	0.01	0.56	0.07	-0.08	-0.01	0.02
window_g	0.01	-0.23	-0.02	0.76	0.68	0.51
window_T	0.00	0.43	0.07	-0.14	-0.04	-0.02
WWR	-0.68	0.77	-0.62	0.36	0.42	-0.27
ventilation_rate	-0.01	-0.12	-0.02	-0.35	0.11	-0.20
shading_depth	-0.07	-0.09	-0.09	-0.34	-0.51	-0.34
Min_temperature	0.00	0.01	0.00	0.00	0.00	0.00

Total order of Sobol

TMY-RCM _Current	Heat release from building (kWh/m² façade)					
Inputs	Opaque	Transparent	Facade	Zone	HVAC	Total
Depth of insulation(U value)	0.19	0.11	0.23	0.25	0.17	0.35
Finishing_Color(solar absorptance)	0.19	0.01	0.22	0.05	0.01	0.15
window_U	0.03	0.28	0.04	0.17	0.12	0.15
window_g	0.03	0.08	0.04	0.39	0.34	0.34
window_T	0.02	0.07	0.02	0.13	0.15	0.14
WWR	0.83	0.71	0.78	0.45	0.39	0.33
ventilation_rate	0.00	0.00	0.00	0.03	0.00	0.00
shading_depth	0.05	0.12	0.07	0.44	0.45	0.45
Min_temperature	0.04	0.10	0.05	0.29	0.17	0.26

TMY-RCM _Current	Total heat release		
inputs	SRC(Positive/negative aspect)	St(absolute value)	SRC*St
Depth of insulation(U value)	1	0.35	0.35
Finishing_Color(solar absorptance)	1	0.15	0.15
window_U	1	0.15	0.15
window_g	1	0.34	0.34
window_T	-1	0.14	-0.14
WWR	-1	0.33	-0.33
ventilation_rate	-1	0.02	-0.02
shading_depth	-1	0.45	-0.45
Min_temperature	1	0.26	0.26

TMY-RCM _Current	Total heat release	
Rank of inputs	Final ranking(sorted inputs)	Ranked value
1(Most important for increasing)	Depth of insulation(U value)	0.35
2	window_g	0.34
3	Min_temperature	0.26
4	Finishing_Color(solar absorptance)	0.15
5	window_U	0.15
6	ventilation_rate	-0.02
7	window_T	-0.14
8	WWR	-0.33
9(Most important for decreasing)	shading_depth	-0.45

Fig. 7. Façade design strategies ranking methodology(Green shading indicates a positive correlation, while red shading indicates a negative correlation with the outcome).

median, the interquartile range, and potential outliers, as illustrated in Fig. 8. It emerges the following aspects. All three models (RCM, Meteonorm, and CCWeatherGen) demonstrate a clear warming trend from current to future periods, with increasing median temperatures. However, they differ significantly in their projections of variability and extreme values. RCM shows the most consistent increase in median temperatures with relatively stable interquartile ranges, while Meteonorm exhibits the largest increase in variability from current to future periods. CCWeatherGen, interestingly, maintains the smallest interquartile ranges across all time steps but presents the most extreme high-temperature outliers, particularly in mid-future projections. This divergence in model behaviour becomes more pronounced in future scenarios, with CCWeatherGen showing the most dramatic increase in extreme high-temperature events. Notably, while all models predict an increase in high-temperature outliers, low-temperature extremes become less severe in future projections across all methods.

These differences can be directly attributed to the distinct mathematical principles underlying each downscaling approach:

The dynamical downscaling approach utilizes a Regional Climate Model (RCM), which employs physics-based numerical models to simulate atmospheric processes at high resolutions [97]. Unlike statistical methods, it directly solves the fundamental equations governing atmospheric dynamics [98]. This physics-based foundation explains why RCM shows the most consistent increase in median temperatures with relatively stable interquartile ranges across time periods. The model maintains physical consistency across all variables and preserves the internal variability of the climate system while capturing non-linear feedback mechanisms [99]. The bias correction procedures applied to RCM outputs primarily adjust systematic biases without significantly altering the variability structure [100].

Meteonorm employs a sophisticated stochastic weather generation approach [101] that combines measured data with interpolation models. For future climate projections, it utilizes a two-step process: first adjusting monthly means according to GCM/RCM projections ($\bar{X}_{m,future} = \bar{X}_{m,present} + \Delta\bar{X}_{m,IPCC}$), then generating synthetic hourly data through stochastic processes ($x_{h,future} = f(\bar{X}_{m,future}, \sigma_{m,future}, P_h)$) where P_h is a stochastic parameter that maintains proper temporal sequencing and cross-correlations between variables. This mathematical structure explains why Meteonorm exhibits the largest increase in variability from current to future periods, as its stochastic approach introduces entirely new patterns of variability based on projected climate statistics [37].

CCWeatherGen uses a "morphing" approach [39] that applies mathematical transformations to historical data. For temperature, it employs a combined shift-and-stretch equation ($x = x_0 + \Delta x_m + a_m(x_0 - \langle x_0 \rangle_m)$) where x is the future variable, x_0 is the present-day value, Δx_m is the absolute monthly change, and a_m is the ratio of monthly variances. This method preserves the temporal sequence of the original data while amplifying extremes, explaining why CCWeatherGen maintains the smallest interquartile ranges across all time steps but presents the most extreme high-temperature outliers, particularly in mid-future projections [102].

To assess the reliability of the dynamically downscaled weather data, observational data from 2006 to 2020 for the Caselle site in Turin, Italy were used as a baseline for comparison. These data, collected by the Piedmont Regional Environmental Protection Agency [66], allowed validation of both raw and bias-adjusted climate outputs. Three key statistical indicators were used in the comparison: the mean bias error

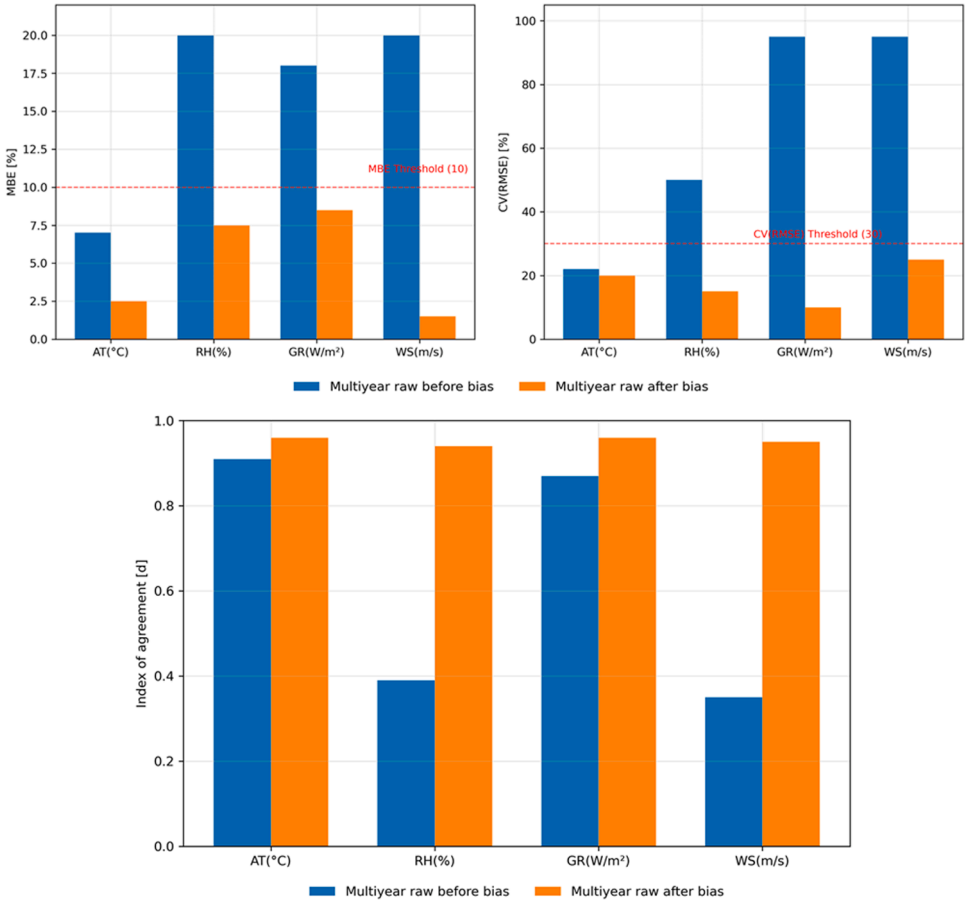

Fig. 9. MBE, CV(RMSE) and Index of agreement (d)Comparison of Multiyear Raw Weather Data with observation before and after Bias-Correction(AT: Air temperature, RH: Relative Humidity, GR: Global solar Radiation, WS: Wind Speed).

(MBE), the coefficient of variation of the root mean square error (CV (RMSE)) as recommended by the ASHRAE guideline [72], and the index of agreement (d) [73]. MBE and CV(RMSE) assess the deviation between simulated and measured values, with acceptable thresholds of ±10 % for MBE and 30 % for CV(RMSE) for hourly data. The agreement index (d) provides a standardized measure of prediction accuracy, ranging from 0 (no agreement) to 1 (perfect agreement) (Fig. 9). While *d* effectively captures both additive and proportional differences between observed and simulated means and variances, it should be noted that it can be sensitive to extreme values due to its use of squared differences.

These statistical indicators were applied to compare both multiyear data before and after bias-adjusted dynamically downscaled data against historical observations, examining air temperature, relative humidity, global solar radiation, and wind speed to evaluate the effectiveness of the bias adjustment process. shows the MBE, CV(RMSE), and index of agreement (d) across all weather parameters. The analysis reveals substantial improvements following bias adjustment across all metrics. Air temperature, which initially showed the best alignment with observations, improved further after bias correction with MBE decreasing from 7 % to 2.5 % and CV(RMSE) reducing from 22 % to 20 %, both well within their respective thresholds. The index of agreement also increased slightly from 0.91 to 0.96, indicating excellent correlation with measured data.

Relative humidity exhibited dramatic improvements, with MBE dropping from 20 % to 7.5 % and CV(RMSE) decreasing from 50 % to 15 %. The most striking improvement was in its index of agreement, which rose from 0.39 to 0.94. Similarly significant improvements were observed in global solar radiation, where MBE reduced from 18 % to 8.5 % and CV(RMSE) decreased substantially from 95 % to approximately 10 %, with the index of agreement improving from 0.87 to 0.96. Wind speed measurements showed remarkable enhancement after bias correction, with MBE decreasing from 20 % to 1.5 % and CV(RMSE) reducing from 95 % to 25 %. The index of agreement showed the most dramatic improvement among all parameters, rising from 0.35 to 0.95. Overall, while only air temperature initially met the MBE threshold of ±10 % before bias correction, all parameters fell well within both MBE and CV(RMSE) thresholds after adjustment. The consistently high post-correction index of agreement values (>0.94) across all parameters further confirms the effectiveness of the bias adjustment process.

Following validation of the effectiveness of the bias adjustment, a comparative analysis was conducted between all-weather file generation methods against observational data using probability density functions (PDF) and cumulative distribution functions (CDF). These statistical distributions are particularly useful for the analysis of climate data, as they allow a comprehensive comparison of data patterns and extremes [74]. While PDFs reveal the frequency distribution and capture the overall shape of the data, CDFs provide insight into the cumulative probability distributions and are particularly valuable for analysing extreme values and percentile-based comparisons.

The comparative analysis (see Appendix 2) shows varying degrees of agreement for different weather parameters. For air temperature, RCM shows the closest agreement with observations in both PDF and CDF distributions, especially in the middle temperature range (10–25 °C), while CCWeatherGen tends to overestimate higher temperatures (>25 °C). Relative humidity distributions show that Meteonorm achieves better agreement with observations, especially in the 40–80 % range, although all methods show some deviation in extreme humidity conditions. Wind speed distributions show good agreement between RCM and observations, both in capturing the predominant low speed conditions (0–4 m/s) and in the distribution of higher wind speeds. For global solar radiation, all methods show reasonable agreement with observations up to 600 W/m^2, but RCM shows superior performance in representing peak radiation values and maintaining consistent distribution patterns across the range. Based on these distribution comparisons, RCM generally shows the most consistent agreement with observational data for all weather parameters, suggesting that it may provide the most reliable basis for future climate projections.

3.2. Reference building thermal resilience indicators

In this part the building thermal resilience KPIs for the reference building characteristics are reported, namely the heat release from building, total delivered energy, peak heating and cooling, and indoor overheating degree for different time step (*Table 5*), in order to understand the variation of performance as far as building thermal resilience is concerned for a building with the minimum local legislative requirements characteristics. The CCWeatherGen method consistently predicts the highest total heat release from the building across all time horizons, with values ranging from 244 kWh/m^2 facade in the current period to 256 kWh/m^2 facade in the future period. Conversely, the RCM method generally shows the lowest heat release values. All methods indicate an increasing trend in total heat release from current to future periods, with the most significant increase observed in the HVAC component. Energy consumption patterns vary among methods, but all show a substantial increase in cooling energy and a decrease in heating energy over time. Peak cooling loads are projected to rise significantly, with CCWeatherGen predicting the highest future cooling peak of 30.73 W/m^2. The IohD shows an upward trend across all methods, with CCWeatherGen projecting the most severe overheating in the future (0.28 °C). Notably, while RCM and Meteonorm methods show similar trends, CCWeatherGen consistently predicts higher values for most indicators, suggesting it may provide more conservative estimates for climate change impacts on building performance.

3.3. Sensitivity analysis

This section presents the results of the analysis for three fundamental aspects of a building's thermal resilience, (i) energy performance (total energy supplied and peak loads), (ii) degree of indoor overheating and (iii) total heat release from the building, for different weather file generation methods over three-time horizons, both in absolute terms and in sensitivity rankings. For each aspect, absolute value comparisons are firstly presented to understand the magnitude and range of predictions for different weather file generation methods. This is followed by a sensitivity analysis that ranks the façade design parameters according to their influence on each performance metric. Finally, the interactions between these different performance aspects is examined, to understand potential trade-offs in façade design decisions.

3.3.1. Energy performance (total delivered energy and peak loads)

The comparison of the absolute values of delivered energy for the different weather file generation methods (Fig. 10) reveals different patterns of energy consumption and variability over time. The percentages shown in box whisker plot represents the relative changes compared with the current period, calculated for both mean and maximum values. While all methods predict an increase in delivered energy from current to future scenarios, they differ significantly in both magnitude and variability. RCM shows the most pronounced increases in mean delivered energy, rising 12 % from current to mid-future and 37 % from current to future periods. The maximum values show even more dramatic increases of 23 % and 46 % respectively, indicating significant potential for extreme energy demand scenarios. RCM also exhibits the highest median values across all time periods, with increasingly wider ranges in future projections. Meteonorm predicts more moderate increases, with mean values rising 12 % by mid-future and 13 % by future periods. Maximum values show increases of 16 % and 33 % respectively. While its median values are lower than RCM's, Meteonorm shows increased variability in both mid-future and future periods, particularly in the upper quartile range. CCWeatherGen demonstrates the most optimistic projections, with mean values increasing by only 6 % in mid-future and 12 % in future periods. Maximum values show increases of 7 % and 23 % respectively. While it maintains the lowest median values

Table 5
Result of benchmark model.

Future weather file types and time horizon		Heat release from building (kWh/m^2 facade)					Delivered Energy (kWh/m^2)				Peak load(W/m^2)		Indoor overheating (°C)
	Time horizon	Opaque	Transparent	Zone	HVAC	Total	Cooling	Heating	Lighting	Total	Heating	Cooling	IohD
RCM	Historical	90.88	17.37	80.66	15.43	204.34	3.22	2.84	6.71	12.77	15.76	16.83	0.11
	Mid future	92.04	16.33	80.34	20.67	209.38	4.31	1.82	6.48	12.61	14.70	18.53	0.10
	Future	91.44	13.14	82.05	30.42	217.05	6.34	0.60	6.59	13.53	13.74	30.23	0.17
CCWeatherGen	Historical	108.36	21.43	95.36	19.41	244.56	4.05	2.10	5.78	11.93	14.43	18.37	0.08
	Mid future	106.78	19.21	93.09	29.09	248.17	6.08	1.71	5.78	13.57	13.72	27.25	0.13
	Future	106.72	17.06	93.37	39.60	256.75	8.26	1.20	5.78	12.24	12.83	30.73	0.28
Meteonorm	Historical	94.97	16.57	79.11	14.88	205.53	3.10	1.38	6.01	10.49	15.85	17.72	0.10
	Mid future	93.91	14.61	77.42	27.84	213.78	5.80	1.31	5.78	12.89	14.90	20.88	0.08
	Future	95.75	12.80	72.96	45.10	226.61	9.40	0.53	5.90	15.83	13.22	23.12	0.19

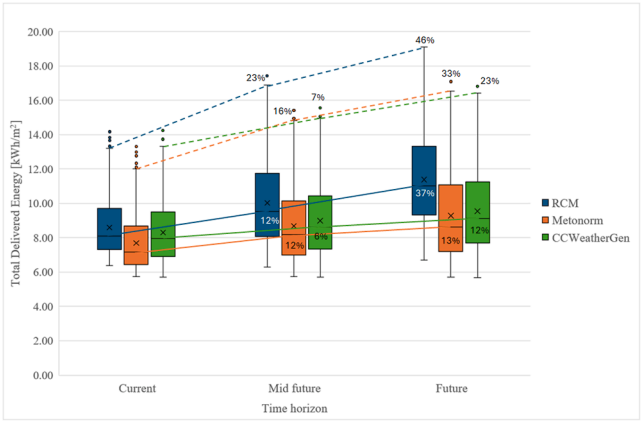

Fig. 10. Box whisker plot of absolute value for delivered energy.

among the methods, CCWeatherGen shows similar patterns of increased variability in future scenarios. The divergence between methods becomes more pronounced in future scenarios, with RCM consistently predicting higher energy demands and greater variability compared to statistical downscaling methods (Meteonorm and CCWeatherGen).

The sensitivity analysis of total EUI (cf. Appendix 1) reveals remarkably consistent rankings of façade design parameters across all weather file generation methods and time horizons. Window g-value consistently emerges as the most influential parameter for increasing EUI, with values ranging from 0.36 to 0.40 across all scenarios. This is closely followed by shading depth (0.32–0.34) and insulation depth (0.27–0.33), showing similar levels of importance across all methods. At the opposite end of the spectrum, WWR consistently ranks as the most significant parameter for decreasing energy consumption, with notably stable values around −0.47 across all methods and time periods. Window transmittance shows the second strongest negative impact, though its influence varies somewhat more across methods (−0.25 to −0.33).

Minor variations between methods are observed in the middle-ranked parameters. For instance, minimum temperature setpoint for natural ventilation shows slightly higher importance in CCWeatherGen (0.26–0.28) compared to other methods, while ventilation rate maintains consistently low influence (0.03–0.05) across all scenarios. External surface finishing (outdoor surface solar absorptance) shows the least impact, with a consistent minimal negative effect (−0.02) across all methods and time periods. The stability of these rankings across different weather file generation methods suggests that key façade design decisions may be robust against uncertainties in future climate projections from an EUI perspective.

The box plots comparing peak heating and cooling loads (Fig. 11) reveal distinct patterns between different weather file generation methods. For peak heating load, all methods show a consistent decreasing trend, though with varying magnitudes. RCM predicts the most moderate decrease (−13 % by future period), while CCWeatherGen shows the most significant reduction (−15 %). The variability between methods is relatively small for heating loads, suggesting reasonable agreement in their projections of future heating demands. In contrast, peak cooling load projections show much greater divergence between methods. CCWeatherGen predicts the most dramatic increases, showing a 70 % increase by mid-future and a striking 110 % increase by the future period. RCM demonstrates a more gradual but still substantial increase, with a 25 % rise by mid-future and 150 % by the future period.

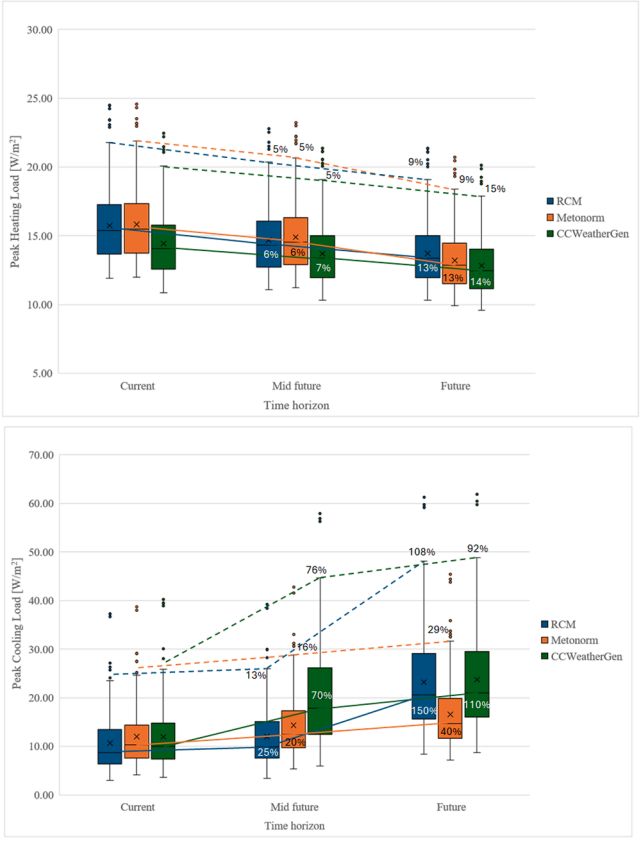

Fig. 11. Box whisker plot of absolute value for Peak heating load (top) and Peak cooling load (bottom).

Meteonorm provides the least conservative cooling projections, showing 20 % and 40 % increases for mid-future and future periods respectively. The variability in cooling load predictions also increases significantly in future periods, with CCWeatherGen showing the widest range of potential values. This comparison reveals that while there is relative consensus among methods regarding the decrease in peak heating loads, there are significant discrepancies in their predictions of future cooling demands. The statistical downscaling method (CCWeatherGen) tends to predict more extreme increases in cooling loads compared to the dynamical downscaling approach (RCM), particularly in the near term, while Meteonorm consistently provides more moderate projections. These differences highlight the importance of considering the correct climate downscaling method when assessing how façade parameters could affect future cooling system requirements.

The sensitivity analysis for peak heating and cooling loads (cf. Appendix 1) reveals distinct patterns of façade parameter influence, with notable differences between heating and cooling performance. For peak heating load, the rankings show remarkable consistency across all weather file generation methods and time horizons, with insulation depth emerging as the dominant parameter for decreasing peak loads (consistent value of −0.92). WWR shows the strongest positive influence, though with a much smaller magnitude (0.13), followed by window U-value (0.08). For peak cooling load, the parameter rankings show more variation both in magnitude and relative importance across different methods and time horizons. Shading depth consistently ranks as the most influential parameter for decreasing peak cooling loads, though its impact varies from −0.53 in current scenarios to −0.41 in future projections using CCWeatherGen. WWR demonstrates the strongest positive influence on peak cooling loads, with values ranging from 0.36 to 0.42, showing slightly increased importance in future scenarios, particularly in CCWeatherGen projections. Window g-value maintains a consistent second position for increasing cooling loads, with its influence strengthening slightly in future scenarios (from 0.27 to 0.31–0.32). The middle-ranked parameters show some variation in their ordering across methods, with minimum temperature setpoint and insulation depth exchanging positions but maintaining similar magnitudes (0.14–0.17). Window transmittance shows a moderate negative impact (−0.12 to −0.14) on peak cooling loads, while finishing colour and ventilation rate demonstrate minimal influence (≤0.01) across all scenarios.

This analysis reveals that while heating load sensitivity is dominated by a single parameter (insulation depth), cooling load performance is influenced by a more complex interaction of multiple façade parameters, with their relative importance showing greater sensitivity to the choice of weather file generation method.

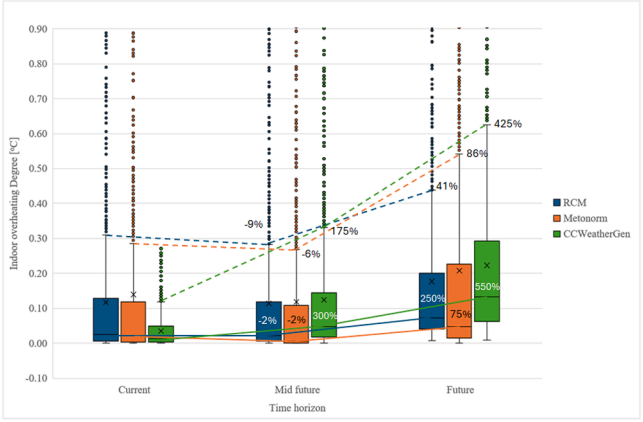

Fig. 12. Box whisker plot of absolute value for indoor overheating degree.

3.3.2. Indoor overheating degree

The comparison of absolute values for Indoor Overheating Degree (IohD) (Fig. 12), reveals significant variations in both magnitude and trends across the different weather file generation methods. CCWeatherGen shows the most dramatic increase in overheating risk, with a substantial jump of 300 % from current to mid-future period, followed by an even more striking 550 % increase in the future period. This method also demonstrates the widest variability in future scenarios, particularly in the upper quartile range.

Meteonorm predicts a more gradual progression of overheating risk, with a slight decrease (−2 %) in the mid-future period followed by a significant increase of 75 % in the future period. The variability in Meteonorm predictions also increases over time, though not as extensively as CCWeatherGen. Notably, Meteonorm shows a higher concentration of outliers in future scenarios, suggesting increased frequency of extreme overheating events. RCM exhibits the most moderate progression, showing a small decrease (−2 %) in the mid-future period followed by a considerable increase of 250 % in the future period. While RCM maintains relatively lower median values compared to CCWeatherGen, it shows consistent increases in variability across time horizons. The divergence between methods becomes particularly pronounced in the future period, where the predicted increases range from 41 % (RCM) to 425 % (CCWeatherGen), highlighting significant uncertainties in long-term overheating projections.

This analysis suggests that while all methods predict increased overheating risk in future scenarios, the magnitude and timing of these increases vary substantially depending on the weather file generation method used, with statistical methods (particularly CCWeatherGen) predicting more severe overheating conditions compared to the dynamical downscaling approach (RCM).

The sensitivity analysis of IohD (cf. Appendix 1) reveals consistent patterns in the ranking of façade design parameters across different weather file generation methods and time horizons, though with some variations in magnitude. WWR consistently emerges as the most influential parameter for increasing overheating risk, with values ranging from 0.48 to 0.56, showing a slight decrease in importance in future scenarios particularly with CCWeatherGen (dropping from 0.53 to 0.48). Window g-value maintains a strong second position for increasing IohD, with remarkably stable values (0.43–0.47) across all methods and time periods. The minimum temperature setpoint for natural ventilation shows moderate importance but with more noticeable variation across methods and time periods (ranging from 0.29 to 0.43), with CCWeatherGen showing the most significant decrease in its influence in future scenarios.

At the other end of the spectrum, shading depth consistently ranks as the most effective parameter for reducing overheating, with values between −0.42 and −0.46, showing relatively stable influence across all scenarios. Window U-value demonstrates the second strongest negative impact, though its influence varies somewhat across methods (−0.17 to −0.25) and shows a slight weakening in future scenarios with CCWeatherGen. Minor parameters such as finishing colour (solar absorptance) and ventilation rate show minimal influence (≤|0.06|) across all scenarios. Window thermal transmittance maintains a consistently low negative impact (−0.08 to −0.11) across all methods and time periods.

This stability in parameter rankings across different weather file generation methods suggests that key design decisions for managing overheating risk may be relatively robust against uncertainties in future climate projections, though the magnitude of their impact vary significantly depending on the chosen weather file generation method.

3.3.3. Total heat release from building

The comparison of absolute values for total heat release from buildings (Fig. 13) reveals distinct patterns across different weather file generation methods, with all methods showing an increasing trend but varying in magnitude and variability. CCWeatherGen consistently predicts the highest heat release values and demonstrates the most

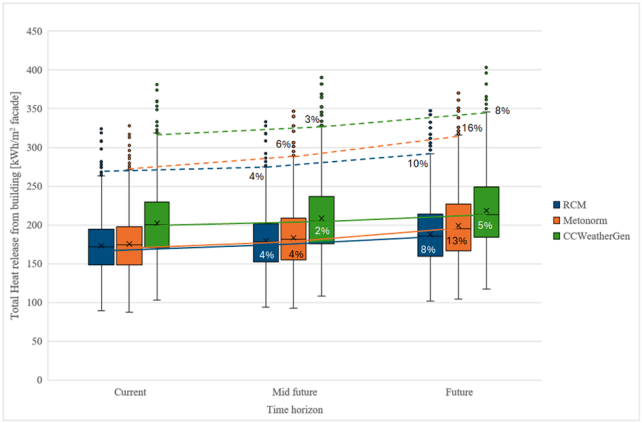

Fig. 13. Box whisker plot of absolute value for heat release from building.

pronounced increase across time horizons. From the current period to mid-future, it shows a 2 % increase, followed by a more substantial 5 % increase in the future period. The method also exhibits the widest interquartile range, particularly in future scenarios, suggesting greater uncertainty in its projections. Meteonorm shows a more moderate progression, with a 4 % increase in the mid-future period followed by a more significant 13 % increase in the future period. While its median values are lower than CCWeatherGen, Meteonorm displays increasing variability in future scenarios, particularly in the upper quartile range. The trend becomes more pronounced in the future period, with outliers reaching higher values.

RCM demonstrates the most optimistic projections for heat release, showing a 4 % increase by mid-future and an 8 % increase by the future period. It maintains the lowest median values among the methods and shows the most consistent variability across time periods. The differences between methods become more pronounced in future scenarios, with maximum values showing particularly wide divergence (8 % for CCWeatherGen versus 10 % for RCM in dashed trend lines). This analysis suggests that while all methods predict increased heat release from buildings over time, the choice of weather file generation method significantly influences both the magnitude of projected increases and the range of potential values, with statistical methods (particularly CCWeatherGen) predicting higher overall heat release compared to the dynamical downscaling approach (RCM).

The sensitivity analysis of total heat release from buildings (cf.Appendix 1) shows some notable variations in parameter rankings across different weather file generation methods and time horizons. The most significant parameters demonstrate a slight shift in relative importance depending on the method used. Window g-value and insulation depth consistently emerge as the two most influential parameters for increasing heat release, though their relative ranking varies. Window g-value shows an increasing trend in importance across time periods (from 0.34–0.36 in current to 0.40–0.43 in future scenarios), particularly in Meteonorm projections. Shading depth consistently ranks as the most effective parameter for decreasing heat release, with values ranging from −0.42 to −0.49, showing slightly stronger influence in CCWeatherGen projections. WWR maintains the second strongest negative impact, though its influence gradually weakens in future scenarios (from −0.30 to −0.36 in current to −0.27 to −0.30 in future periods). The middle-ranked parameters show relatively stable influences across methods and time periods. Minimum temperature setpoint maintains consistent moderate importance (0.25–0.28), while window U-value and finishing colour (solar absorptance) show similar levels of influence (0.11–0.17). Window solar transmittance demonstrates a moderate negative impact that slightly increases in future scenarios (−0.14 to −0.17). Ventilation rate shows minimal influence (−0.01 to −0.02) across all scenarios, indicating its relatively minor role in total heat release. The stability of most parameter rankings across different weather file generation methods suggests that key design decisions for managing building heat release may be relatively robust against uncertainties in future climate projection generation, though the magnitude of their impact shows some sensitivity to the chosen downscaling method.

3.4. Interaction between the KPIs

To explore how façade design parameters simultaneously affect multiple dimensions of thermal resilience, a comparative visualization framework was developed, examining the interactions between pairs of KPIs. The analysis positions façade parameters in a four-quadrant plot based on their final ranking values for each KPI across different time horizons. Each quadrant represents a distinct impact pattern: parameters can simultaneously increase or decrease both KPIs (upper right and lower left quadrants respectively) or show opposing effects by increasing one KPI while decreasing the other (upper left and lower right quadrants). This visualization approach could reveal complex trade-offs between different thermal resilience objectives and could help identifying façade design strategies that offer synergistic benefits or require careful balance between competing performance goals (Fig. 14).

The comparative analysis between pairs of KPIs reveals both consistent patterns and notable variations across different weather file generation methods and time horizons. For the IohD-EUI relationship (Fig. 15), window g-value and depth of insulation consistently appear in the upper right quadrant across all weather types, indicating these parameters simultaneously increase both overheating risk and energy consumption. CCWeatherGen (green markers) predicts more extreme effects for these parameters, with increasing spread between current and future scenarios (indicated by marker size). In contrast, RCM (blue markers) shows more conservative predictions with tighter clustering. WWR shows strong positive correlation with overheating while reducing energy use (lower right quadrant), with CCWeatherGen showing greater divergence from other methods in future scenarios, suggesting increasing uncertainty in long-term predictions.

The IohD-HR interaction (Fig. 16) shows different parameter behaviours and temporal evolution patterns. Shading depth emerges as a particularly effective strategy, appearing in the lower left quadrant where it reduces both overheating and heat release, with a remarkably consistent positioning across all methods and time horizons (tight

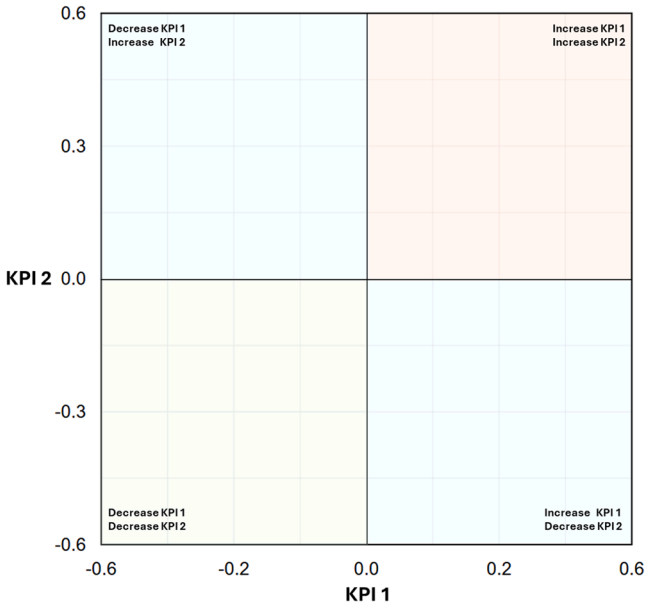

Fig. 14. KPI Interaction Matrix.

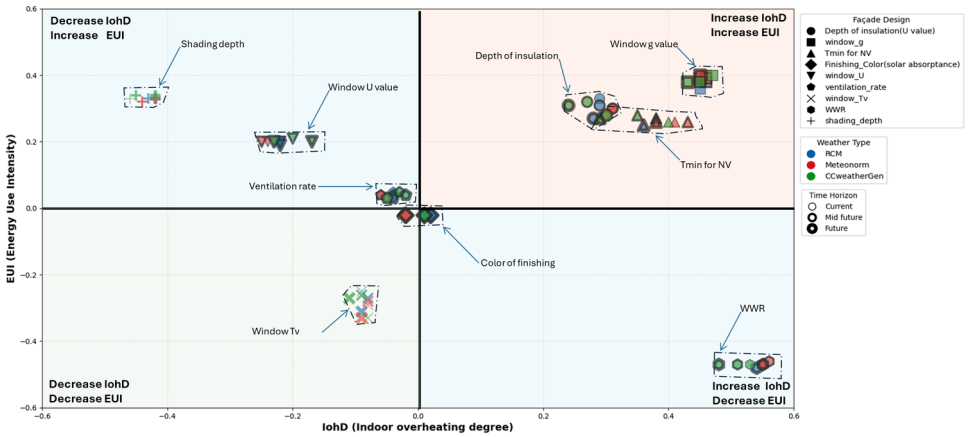

Fig. 15. IohD vs EUI.

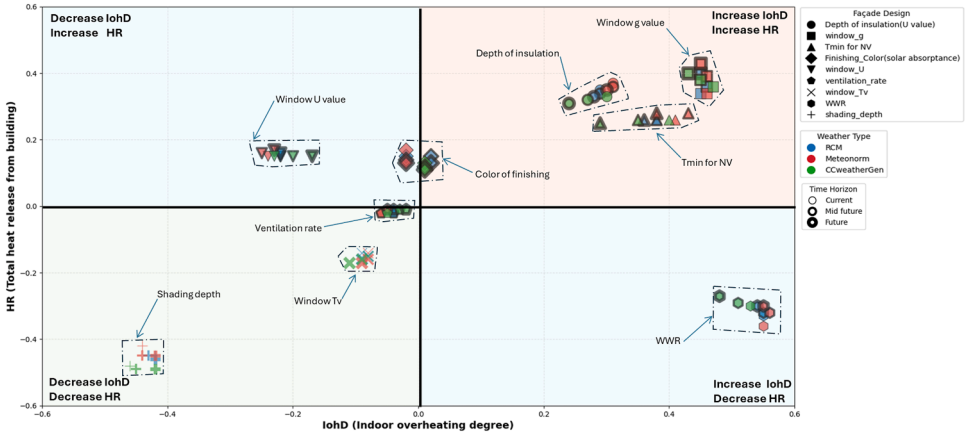

Fig. 16. IohD vs HR.

clustering of markers). The window g-value maintains its position in the upper right quadrant, with CCWeatherGen predicting stronger effects in future scenarios compared to RCM and Meteonorm. The minimum temperature setpoint for natural ventilation (Tmin for NV) shows an increasing spread between the methods in future scenarios (being particularly sensitive to outdoor air temperature), particularly in the CCWeatherGen predictions, indicating growing uncertainty in its long-term effects.

The relationship between EUI and HR (Fig. 17) highlights additional complexities and temporal patterns in façade design optimization. Window transmittance (window_Tv) appears in the lower left quadrant, offering simultaneous benefits for both energy efficiency and urban heat island mitigation, with moderate spread between methods but consistent relative positions across time horizons. The finishing colour (solar absorptance) demonstrates remarkably consistent behaviour across all methods and time horizons, as evidenced by the tight clustering of markers regardless of whether file type or temporal period. Window g-value and depth of insulation show the greatest methodological divergence in this comparison, with CCWeatherGen predicting stronger positive correlations in future scenarios.

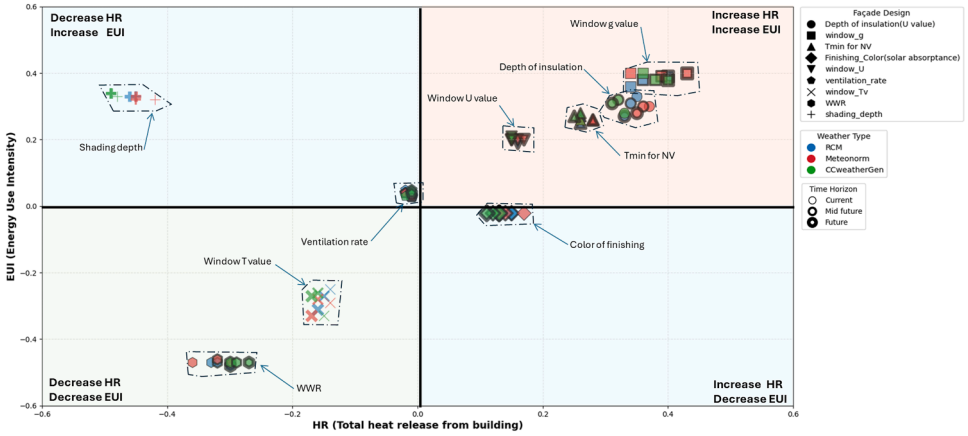

Fig. 17. EUI vs HR.

4. Discussion

This study investigates how different weather file generation methods influence façade design decisions for climate-resilient buildings, focusing on a south-facing office space in Turin. The analysis reveals significant methodological differences that are both consistent with and extend previous findings [24,44,37] particularly regarding the impact of downscaling approaches on performance predictions and design strategy effectiveness. These analysis demonstrates substantial variations in absolute predictions between downscaling methods, confirming earlier findings by Escandón et al. [24]. who reported variations up to 18 % in thermal performance metrics between methods. RCM consistently produces more optimistic predictions with tighter parameter clustering, while CCWeatherGen predicts more extreme effects with greater spread in future scenarios, particularly in overheating predictions, aligning with observations by Tootkaboni et al. [44] regarding statistical downscaling methods. This methodological divergence becomes especially relevant when considering findings from Moazami et al. [37] about the impact of future weather data typology on building performance.

The distinct mathematical principles and assumptions underlying each downscaling method directly influence their predictions of building thermal resilience KPIs. The physics-based approach of RCM, which preserves internal climate variability and physical relationships between variables, yields more moderate increases in extreme-condition KPIs such as overheating degree (250 % increase by 2080) and tends to predict lower heat release values but higher energy consumption. CCWeatherGen's morphing technique, which mathematically amplifies deviations from monthly means, systematically produces more extreme projections for overheating risk (550 % increase by 2080) and peak cooling loads (110 % increase by 2050). This amplification effect directly stems from the shift-and-stretch equation that exaggerates historical extremes. Meteonorm's stochastic approach, by generating entirely new weather patterns based on adjusted statistical parameters, creates more variable interquartile ranges in future scenarios but produces more conservative projections for peak cooling loads (40 % increase by 2080). These methodological distinctions explain why CCWeatherGen consistently predicts higher heat release values across all time horizons, while RCM shows more consistent variability in future scenarios, reflecting its preservation of atmospheric physics relationships.

The comparative ranking analysis reveals complex interactions between façade parameters and thermal resilience indicators. While window g-value and insulation depth consistently rank as crucial factors across methods, supporting findings from Tettey et al. [48]. and Karimpour et al. [49]., their predicted impact varies significantly by method. For instance, the increased influence of window g-value in CCWeatherGen future scenarios aligns with Passer et al.'s [54] observations about solar control importance in future climates, though the analysis suggests this effect may be overestimated by statistical downscaling methods. Cross-KPI analysis reveals complex interactions between facade parameters and different aspects of thermal resilience, identifying strategies with varying degrees of effectiveness and trade-offs. External shading (herewith represented by an increasing shading depth) emerges as one of the most robust strategies, reducing both overheating risk (41–46 % decrease in IohD) and heat release (42–49 % reduction) while maintaining acceptable energy performance across all weather file methods. This extends findings from Zhang et al. [50]. about solar control importance by demonstrating effectiveness across multiple performance domains. Conversely, transparent building envelope characteristics present notable performance conflicts - increased WWR reduces energy consumption through improved daylighting and decreased heating demand (up to 47 % reduction in total energy use, with heating energy reductions of approximately 15–20 %) but simultaneously increases overheating risk (48–56 % higher IohD) and heat release to urban environment (30–36 % increase). The magnitude of these trade-offs varies significantly between downscaling methods, with statistical approaches like CCWeatherGen predicting more extreme impacts than RCM, extending observations by Krelling et al. [51] about the importance of comprehensive strategy evaluation in future climate scenarios.

The analysis of interactions between KPIs in this study focuses on pairwise comparisons to identify key trade-offs in facade design decisions. This approach reveals important conflicts, such as how increased WWR reduces energy consumption through improved daylighting and decreased heating demand (up to 47 % reduction in total energy use) but simultaneously increases overheating risk (48–56 % higher IohD) and heat release to the urban environment (30–36 % increase). Similarly, it was observed that shading depth consistently reduces both overheating and heat release (41–46 % decrease in IohD and 42–49 % reduction in heat release) but can increase heating energy demand during winter months. While these pairwise comparisons capture critical design trade-offs, a fully systematic exploration examining all KPI combinations simultaneously would require a multidimensional approach beyond the scope of this paper's primary focus on weather file generation methods. Future research could expand the present methodological framework to include comprehensive multi-KPI analysis, potentially revealing additional facade design optimization opportunities that balance competing performance objectives across the full spectrum of thermal resilience indicators.

The temporal evolution (from current to future climate scenarios) of building envelope strategy effectiveness reveals that increased insulation depth consistently improves current energy performance (92 % reduction in peak heating loads), but its future effectiveness varies significantly between methods. For cooling performance, increased insulation depth shows a moderate negative impact, increasing peak cooling loads by 14–17 % across the different methods, with this effect becoming more pronounced in future scenarios. This cooling penalty occurs because higher insulation levels can trap heat within the building during warm periods, increasing cooling demands. CCWeatherGen predicts potential negative impacts on overheating in future scenarios, contradicting the findings of Sehizadeh and Ge [103] of insulation benefits over multiple performance aspects. This highlights the complex trade-offs in insulation strategies, where optimizing for one season (heating) may create challenges in another (cooling), an effect that becomes more critical in future warmer climate scenarios. Similarly, selective glazing technologies show increasing importance in future scenarios across all methods, with the influence of window g-values on overheating (increasing from 0.43 to 0.47 for RCM) and on energy use (0.36 to 0.39 for RCM), supporting the observations of Passer et al. [54], with a consistent influence of factors influencing daylight in the indoor space in terms of energy use (such as window visible transmission and WWR), but suggesting that more nuanced considerations are needed. The impact of shading strategies becomes increasingly important in future scenarios [52,53], with these analysis revealing significant variations in predicted effectiveness across downscaling methods. Detailed statistical comparisons of the weather files (see Figure 18. in Appendix 2) show that CCWeatherGen predicts higher air temperatures, particularly above 25 °C, and exhibits distinct patterns in global solar radiation distribution compared to both observations and RCM. While RCM maintains closer alignment with observed solar radiation patterns, CCWeatherGen shows greater deviation in both intensity and frequency of peak solar conditions. These fundamental differences in how the methods characterize solar radiation and temperature extremes directly affect shading performance predictions - CCWeatherGen higher-intensity solar radiation projections result in shading depth showing up to 15 % greater impact on overheating reduction compared to RCM projections. This methodological distinction extends Amaripadath et al.'s [54] findings on passive cooling strategies by demonstrating how the underlying differences in weather data generation techniques substantially influence the predicted effectiveness of solar control measures.

The analysis also challenges some common assumptions about facade design priorities. External surface solar absorptance shows minimal influence ($\leq|0.06|$) across all KPIs and methods, suggesting it may be less critical for early-stage decisions. Natural ventilation effectiveness varies significantly between methods, with CCWeatherGen projecting more extreme adaptation needs (temperature setpoint influence increasing from 0.29 to 0.43 in terms of Sobol total index) compared to RCM's more moderate projections. This methodological divergence extends findings from Moazami et al. [37] about weather file typology impacts, highlighting the importance of considering multiple climate projection approaches when evaluating adaptive strategies.

From an architectural perspective, these findings offer valuable insights for façade design practitioners working on early-stage conceptual designs. The relative consistency in ranking of façade design strategies across different weather file generation methods suggests that architects can confidently prioritize certain design decisions—such as solar control measures and ventilation strategies—regardless of the specific climate data methodology employed. This provides a degree of certainty in early design phases when decisions about building form, orientation, and envelope configuration have outsized impacts on long-term building performance, as documented by Salvati and Kolokotroni (2023) [46]. Nevertheless, practitioners should remain aware that the absolute performance values predicted by different weather file methods vary significantly, which has implications for compliance-based performance targets and system sizing decisions. As demonstrated by De Masi et al. (2021) [64], practitioners working in temperate climates similar to Turin should be particularly attentive to solar control measures, as these consistently emerge as critical design parameters across all methodologies and performance indicators evaluated in this study.

The study's strength lies in its comprehensive methodology combining multiple downscaling approaches, building on and extending previous methodological frameworks [90,91,54]. Looking toward future research needs, several limitations of the current study should be addressed. The analysis's focus on a single orientation (South) and location (Turin) limits generalizability, particularly given findings by Ji et al. [52] about orientation importance in thermal resilience. The exclusion of urban heat island effects, identified as crucial by Soudian and Berardi [58], and focus on RCP 8.5 scenario constrain the findings' broader applicability to less severe scenarios, while representing a plausible worst-case condition that may delineate system failure thresholds. In addition, while the study provides a robust analysis of thermal resilience, it does not address aspects of hygrothermal performance. This was a deliberate methodological choice based on scientific evidence that in temperate climates (class C), thermal metrics show 3–4 times greater sensitivity to weather file generation methods than hygrothermal metrics (as quantified by [104]). Schroderus et al. (2025) [105] showed that hygrothermal damage functions show minimal variation (<8 %) between different weather file generation methods, while thermal parameters vary by up to 42 %. Nevertheless, hygrothermal aspects remain important considerations for thermal comfort related aspects, but also for building envelope durability, moisture management and indoor air quality under changing climate conditions. Future research could certainly extend the presented methodological approach to more complex building models, investigating whether the patterns identified in this study persist in multi-zone scenarios with more realistic internal loads and HVAC interactions. This would represent a valuable next step in building upon the foundation established in the current study. Subsequent studies should expand this framework to include multiple orientations, building types, and climate zones [56,57], while incorporating urban heat island effects on F-TMY projections to provide more comprehensive design guidance for climate-resilient buildings.

5. Conclusions

This study investigated how different weather file generation methods influence façade design decisions for climate-resilient buildings, examining both absolute value and comparative rankings of design strategies. This analysis of thermal resilience explored three fundamental domains: energy performance (EUI and peak heating and cooling loads), indoor thermal discomfort (IohD), and urban heat impact (total heat release from the building). In absolute terms, significant variations were found between statistical and dynamical downscaling methods. CCWeatherGen consistently predicted more extreme conditions, showing up to 550 % increase in overheating risk (IohD) by 2080, compared to RCM's more moderate 250 % increase. Similarly, for peak cooling loads, CCWeatherGen projected a 110 % increase by 2080, while RCM showed a 150 % increase and Meteonorm predicted only 40 % increase. These methodological differences became particularly pronounced in future scenarios, with variations in predicted increases ranging from 41 % (RCM) to 425 % (CCWeatherGen) for overheating risk.

However, when examining the comparative influence of façade design parameters through sensitivity analysis, rankings remained relatively consistent across weather file methods. Window g-value (0.36–0.40) and shading depth (0.32–0.34) consistently emerged as the most influential parameters for energy performance and overheating risk, while WWR showed the strongest impact on overheating risk (0.48–0.56) across all methods. Insulation depth demonstrated significant importance, particularly for peak heating load reduction (consistent value of −0.92), though its impact on overheating varied between methods. External surface solar absorptance (finishing colour) showed minimal influence ($\leq|0.06|$) across all KPIs and methods, suggesting it may be less critical for early-stage design decisions. The analysis revealed important trade-offs - for instance, increased WWR reduces energy consumption through improved daylighting but increases overheating risk (48–56 % higher IohD). Similarly, external shading demonstrates contrasting effects: while it significantly reduces both overheating risk (41–46 % decrease) and heat release to the urban environment (42–49 % reduction), it can increase heating energy demand during winter months, particularly affecting peak heating loads (up to 15 % increase).

These findings demonstrate that while different weather file generation methods can significantly affect absolute performance predictions, within this temperature climate they maintain consistent rankings of façade design strategies' effectiveness. This suggests that early-stage design decisions about relative priority of different façade parameters may be robust against uncertainties in future climate projections, even though absolute performance targets may need careful consideration of methodological differences. Despite different limitations, such as the focus on a single orientation and location, and the need for future work to incorporate multiple emission pathways, the demonstrated methodology provides a structured approach for evaluating façade design decisions under climate change, while highlighting the importance of considering methodological influences on performance predictions.

CRediT authorship contribution statement

Milad Heiranipour: Visualization, Methodology, Data curation, Writing – review & editing, Validation, Investigation, Conceptualization, Writing – original draft, Software, Formal analysis. **Miren Juaristi:** Resources, Conceptualization, Writing – review & editing, Project administration, Supervision, Funding acquisition. **Stefano Avesani:** Resources, Conceptualization, Writing – review & editing, Project administration, Supervision, Funding acquisition. **Fabio Favoino:** Visualization, Project administration, Conceptualization, Supervision, Methodology, Writing – review & editing, Resources, Funding acquisition.

Declaration of competing interest

The authors declare no conflicts of interest regarding the publication

of this research.

Acknowledgment

This publication was produced while attending the PhD program in PhD in Sustainable Development And Climate Change at the University School for Advanced Studies IUSS Pavia, Cycle XXXVIII, with the support of a scholarship co-financed by the Ministerial Decree no. 352 of 9th April 2022, based on the PNRR - funded by the European Union - NextGenerationEU - Mission 4 "Education and Research", Component 2 "From Research to Business", Investment 3.3, and by the EURAC Research. We extend our heartfelt gratitude to Dr. Mamak Pourabdollahtootkaboni, Prof. Vincenzo Corrado, and Prof. Ilaria Ballarini for their invaluable contribution to the Weather Data Subtask of IEA EBC Annex 80 - Resilient Cooling of Buildings. Their generous sharing of the code for dynamical downscaling has greatly enhanced our research efforts.

Supplementary materials

Supplementary material associated with this article can be found, in the online version, at doi:10.1016/j.buildenv.2025.113459.

Data availability

Data will be made available on request.

References

[1] Intergovernmental Panel on Climate Change (IPCC), Climate Change 2022 – Impacts, Adaptation and Vulnerability, Cambridge University Press, 2023, https://doi.org/10.1017/9781009325844.
[2] T. Frank, Climate change impacts on building heating and cooling energy demand in Switzerland, Energy Build. 37 (11) (Nov. 2005) 1175–1185, https://doi.org/10.1016/j.enbuild.2005.06.019.
[3] A. Fouillet, et al., Excess mortality related to the August 2003 heat wave in France, Int. Arch. Occup. Env. Health 80 (1) (Sep. 2006) 16–24, https://doi.org/10.1007/s00420-006-0089-4.
[4] D. Barriopedro, R. García-Herrera, C. Ordóñez, D.G. Miralles, S. Salcedo-Sanz, Heat waves: physical understanding and scientific challenges, Rev. Geophys. 61 (2) (Jun. 2023), https://doi.org/10.1029/2022RG000780.
[5] N. Nakicenovic et al., "Special report on emissions scenarios," 2000.
[6] M. Romanello, et al., The 2021 report of the Lancet countdown on health and climate change: code red for a healthy future, Lancet 398 (10311) (Oct. 2021) 1619–1662, https://doi.org/10.1016/S0140-6736(21)01787-6.
[7] E.A.-S. Mayrhuber, et al., Vulnerability to heatwaves and implications for public health interventions – A scoping review, Env. Res 166 (Oct. 2018) 42–54, https://doi.org/10.1016/j.envres.2018.05.021.
[8] R. Basu, High ambient temperature and mortality: a review of epidemiologic studies from 2001 to 2008, Environ. Health 8 (1) (Dec. 2009) 40, https://doi.org/10.1186/1476-069X-8-40.
[9] A. Bunker, et al., Effects of air temperature on climate-sensitive mortality and morbidity outcomes in the elderly; a systematic review and meta-analysis of epidemiological evidence, EBioMedicine 6 (Apr. 2016) 258–268, https://doi.org/10.1016/j.ebiom.2016.02.034.
[10] T. Benmarhnia, S. Deguen, J.S. Kaufman, A. Smargiassi, Review article, Epidemiology 26 (6) (Nov. 2015) 781–793, https://doi.org/10.1097/EDE.0000000000000375.
[11] C.J. Gronlund, A. Zanobetti, J.D. Schwartz, G.A. Wellenius, M.S. O'Neill, Heat, heat waves, and hospital admissions among the elderly in the United States, 1992–2006, Env. Health Perspect. 122 (11) (Nov. 2014) 1187–1192, https://doi.org/10.1289/ehp.1206132.
[12] S. Sun, et al., The influence of pre-existing health conditions on short-term mortality risks of temperature: evidence from a prospective Chinese elderly cohort in Hong Kong, Env. Res 148 (Jul. 2016) 7–14, https://doi.org/10.1016/j.envres.2016.03.012.
[13] J. Cheng, et al., Cardiorespiratory effects of heatwaves: a systematic review and meta-analysis of global epidemiological evidence, Env. Res 177 (Oct. 2019) 108610, https://doi.org/10.1016/j.envres.2019.108610.
[14] A. Hansen, L. Bi, A. Saniotis, M. Nitschke, Vulnerability to extreme heat and climate change: is ethnicity a factor? Glob. Health Action 6 (1) (Dec. 2013) 21364 https://doi.org/10.3402/gha.v6i0.21364.
[15] B.M. Jesdale, R. Morello-Frosch, L. Cushing, The racial/ethnic distribution of heat risk–related land cover in relation to residential segregation, Env. Health Perspect. 121 (7) (Jul. 2013) 811–817, https://doi.org/10.1289/ehp.1205919.
[16] K. Riley, H. Wilhalme, L. Delp, D. Eisenman, Mortality and morbidity during extreme heat events and prevalence of outdoor work: an analysis of community-level data from Los Angeles County, California, Int. J. Env. Res. Public Health 15 (4) (Mar. 2018) 580, https://doi.org/10.3390/ijerph15040580.
[17] H. Honda, K. Iwata, Personal protective equipment and improving compliance among healthcare workers in high-risk settings, Curr. Opin. Infect. Dis. 29 (4) (Aug. 2016) 400–406, https://doi.org/10.1097/QCO.0000000000000280.
[18] J. Klenk, C. Becker, K. Rapp, Heat-related mortality in residents of nursing homes, Age Ageing 39 (2) (Mar. 2010) 245–252, https://doi.org/10.1093/ageing/afp248.
[19] M. Stafoggia, et al., Vulnerability to heat-related mortality, Epidemiology 17 (3) (May 2006) 315–323, https://doi.org/10.1097/01.ede.0000208477.36665.34.
[20] C. Symon, Climate change: action, trends and implications for business, in: The IPCC's Fifth Assessment Report, 1, Working Group, 2013.
[21] A. Sengupta, D. Al Assaad, M. Steeman, H. Breesch, Thermal resilience to overheating assessment in a Belgian educational building with passive cooling strategies during heatwaves and power outages, in: E3S Web of Conferences, EDP Sciences, 2023 01018.
[22] T. Hong, et al., Ten questions concerning thermal resilience of buildings and occupants for climate adaptation, Build. Env. 244 (Oct. 2023) 110806, https://doi.org/10.1016/j.buildenv.2023.110806.
[23] S.H. Holmes, Resilient design modeling: where are we and where can we go?. Climate Adaptation and Resilience Across Scales Routledge, 2021, pp. 6–34.
[24] R. Escandón, C.M. Calama-González, A. Alonso, R. Suárez, Á.L. León-Rodríguez, How do different methods for generating future weather data affect building performance simulations? A comparative analysis of Southern Europe, Buildings 13 (9) (2023) 2385.
[25] I. IPCC, Climate Change 2014: Synthesis report. Contribution of Working Groups I, II and III to the Fifth Assessment Report of the Intergovernmental Panel On Climate Change, IPCC Geneva, Switzerland, 2014.
[26] D.P. van Vuuren, et al., The representative concentration pathways: an overview, Clim. Change 109 (1–2) (Nov. 2011) 5–31, https://doi.org/10.1007/s10584-011-0148-z.
[27] T. Kesik, W. O'brien, A. Ozkan, Toward a standardized framework for thermal resilience modelling and its practical application to futureproofing, Sci. Technol. Built. Env. 28 (6) (Jul. 2022) 742–756, https://doi.org/10.1080/23744731.2022.2043069.
[28] S. Trzaska, E. Schnarr, A review of downscaling methods for climate change projections, U. S. Agency Int. Dev. Tetra. Tech. ARD (September) (2014) 1–42.
[29] D.P. Dee, et al., The ERA-interim reanalysis: configuration and performance of the data assimilation system, Q. J. R. Meteorol. Soc. 137 (656) (2011) 553–597.
[30] M. Herrera, et al., A review of current and future weather data for building simulation, Build. Serv. Eng. Res. Technol. 38 (5) (Sep. 2017) 602–627, https://doi.org/10.1177/0143624417705937.
[31] A.F. Prein, et al., Importance of regional climate model grid spacing for the simulation of heavy precipitation in the Colorado headwaters, J. Clim. 26 (13) (2013) 4848–4857.
[32] Y. Yang, K. Javanroodi, V.M. Nik, Climate change and energy performance of European residential building stocks – A comprehensive impact assessment using climate big data from the coordinated regional climate downscaling experiment, Appl. Energy 298 (Sep. 2021) 117246, https://doi.org/10.1016/j.apenergy.2021.117246.
[33] M. Hosseini, A. Bigtashi, B. Lee, Generating future weather files under climate change scenarios to support building energy simulation – A machine learning approach, Energy Build. 230 (Jan. 2021) 110543, https://doi.org/10.1016/j.enbuild.2020.110543.
[34] V.M. Nik, A.S. Kalagasidis, E. Kjellström, Statistical methods for assessing and analysing the building performance in respect to the future climate, Build. Env. 53 (2012) 107–118.
[35] L.P. Seaby, J.C. Refsgaard, T.O. Sonnenborg, S. Stisen, J.H. Christensen, K. H. Jensen, Assessment of robustness and significance of climate change signals for an ensemble of distribution-based scaled climate projections, J. Hydrol. (Amst.) 486 (2013) 479–493.
[36] S. Belcher, J. Hacker, D. Powell, Constructing design weather data for future climates, Build. Serv. Eng. Res. Technol. 26 (1) (Feb. 2005) 49–61, https://doi.org/10.1191/0143624405bt112oa.
[37] A. Moazami, V.M. Nik, S. Carlucci, S. Geving, Impacts of future weather data typology on building energy performance—Investigating long-term patterns of climate change and extreme weather conditions, Appl. Energy 238 (Mar. 2019) 696–720, https://doi.org/10.1016/j.apenergy.2019.01.085.
[38] V.M. Nik, Making energy simulation easier for future climate—Synthesizing typical and extreme weather data sets out of regional climate models (RCMs), Appl. Energy 177 (2016) 204–226.
[39] M.F. Jentsch, P.A.B. James, and A.S. Bahaj, "CCWeatherGen software: manual for CCWeatherGen climate change weather file generator," 2009.
[40] J. Remund, S. Kunz, METEONORM: global meteorological database for solar energy and applied climatology, Meteotest (1997).
[41] L. Guan, Preparation of future weather data to study the impact of climate change on buildings, Build. Env. 44 (4) (Apr. 2009) 793–800, https://doi.org/10.1016/j.buildenv.2008.05.021.
[42] M.R. Gaterell, M.E. McEvoy, The impact of climate change uncertainties on the performance of energy efficiency measures applied to dwellings, Energy Build. 37 (9) (2005) 982–995.
[43] D. Xia, W. Xie, J. Guo, Y. Zou, Z. Wu, Y. Fan, Building thermal and energy performance of subtropical terraced houses under future climate uncertainty, Sustainability 15 (16) (Aug. 2023) 12464, https://doi.org/10.3390/su151612464.

[44] M.P. Tootkaboni, I. Ballarini, M. Zinzi, V. Corrado, A comparative analysis of different future weather data for building energy performance simulation, Climate 9 (2) (2021) 37.
[45] C.N. Nielsen, J. Kolarik, Utilization of climate files predicting future weather in dynamic building performance simulation–A review, in: Journal of Physics: Conference Series, IOP Publishing, 2021 012070.
[46] A. Salvati, M. Kolokotroni, Urban microclimate and climate change impact on the thermal performance and ventilation of multi-family residential buildings, Energy Build. 294 (Sep. 2023) 113224, https://doi.org/10.1016/j.enbuild.2023.113224.
[47] I. Farrou, M. Kolokotroni, M. Santamouris, Building envelope design for climate change mitigation: a case study of hotels in Greece, Int. J. Sustain. Energy 35 (10) (2016) 944–967.
[48] U.Y.A. Tettey, A. Dodoo, L. Gustavsson, Energy use implications of different design strategies for multi-storey residential buildings under future climates, Energy 138 (Nov. 2017) 846–860, https://doi.org/10.1016/j.energy.2017.07.123.
[49] M. Karimpour, M. Belusko, K. Xing, J. Boland, F. Bruno, Impact of climate change on the design of energy efficient residential building envelopes, Energy Build. 87 (Jan. 2015) 142–154, https://doi.org/10.1016/j.enbuild.2014.10.064.
[50] C. Zhang, et al., Resilient cooling strategies – A critical review and qualitative assessment, Energy Build. 251 (Nov. 2021) 111312, https://doi.org/10.1016/j.enbuild.2021.111312.
[51] A.F. Krelling, R. Lamberts, J. Malik, W. Zhang, K. Sun, T. Hong, Defining weather scenarios for simulation-based assessment of thermal resilience of buildings under current and future climates: a case study in Brazil, Sustain. Cities Soc. 107 (Jul. 2024) 105460, https://doi.org/10.1016/j.scs.2024.105460.
[52] L. Ji, C. Shu, A. Laouadi, M. Lacasse, L.(Leon) Wang, Quantifying improvement of building and zone level thermal resilience by cooling retrofits against summertime heat events, Build. Env. 229 (Feb. 2023) 109914, https://doi.org/10.1016/j.buildenv.2022.109914.
[53] D. Amaripadath, M.Y. Joshi, M. Hamdy, S. Petersen Jr., B. Stone, S. Attia, Thermal resilience in a renovated nearly zero-energy dwelling during intense heat waves, J. Build. Perform. Simul. (Sep. 2023) 1–20, https://doi.org/10.1080/19401493.2023.2253460.
[54] A. Passer, C. Ouellet-Plamondon, P. Kenneally, V. John, G. Habert, The impact of future scenarios on building refurbishment strategies towards plus energy buildings, Energy Build. 124 (Jul. 2016) 153–163, https://doi.org/10.1016/j.enbuild.2016.04.008.
[55] A. Sehizadeh, H. Ge, Impact of future climate change on the overheating of Canadian housing retrofitted to the PassiveHaus standard: a case study, in: Proceedings of the eSim, 2014.
[56] M. Sheng, M. Reiner, K. Sun, T. Hong, Assessing thermal resilience of an assisted living facility during heat waves and cold snaps with power outages, Build. Env. 230 (Feb. 2023) 110001, https://doi.org/10.1016/j.buildenv.2023.110001.
[57] L. Sanchez, P. Mathew, L.S. Hoon, and W. Travis, "Developing and evaluating a metric for office building energy resilience during a power outage," 2023.
[58] S. Soudian, U. Berardi, Impact of future climate scenarios on thermal performance and resilience of building façades: canadian climate case study, Build. Env. 267 (Jan. 2025) 112245, https://doi.org/10.1016/j.buildenv.2024.112245.
[59] D. Amaripadath, P.A. Mirzaei, S. Attia, Multi-criteria thermal resilience certification scheme for indoor built environments during heat waves, Energy Built Environ. (May 2024), https://doi.org/10.1016/j.enbenv.2024.05.001.
[60] T. Felix Kriesten, A. Ziemann, V. Goldberg, C. Schünemann, The effect of regional, urban and future climate on indoor overheating – A simplified approach based on measured weather data, statistical evaluation, and urban climate effects for building performance simulations, City Environ. Interact. 24 (Dec. 2024) 100163, https://doi.org/10.1016/j.cacint.2024.100163.
[61] Z. Duan, P. de Wilde, S. Attia, J. Zuo, Challenges in predicting the impact of climate change on thermal building performance through simulation: a systematic review, Appl. Energy 382 (Mar. 2025) 125331, https://doi.org/10.1016/j.apenergy.2025.125331.
[62] E.E. Agency, Climate change, impacts and vulnerability in Europe 2016—An indicator-based report, Publ. Off. (2017), https://doi.org/10.2800/534806.
[63] L. Pierangioli, G. Cellai, R. Ferrise, G. Trombi, M. Bindi, Effectiveness of passive measures against climate change: case studies in Central Italy, Build. Simul. 10 (4) (Aug. 2017) 459–479, https://doi.org/10.1007/s12273-016-0346-8.
[64] R.F. De Masi, A. Gigante, S. Ruggiero, G.P. Vanoli, Impact of weather data and climate change projections in the refurbishment design of residential buildings in cooling dominated climate, Appl. Energy 303 (Dec. 2021) 117584, https://doi.org/10.1016/j.apenergy.2021.117584.
[65] M. Heiranipour, M. Juaristi, S. Avesani, F. Favoino, and V. Serra, "Contrasting building performance and thermal resiliency: a simulation-based quantitative evaluation framework for evaluating the impact of building envelope technologies," 2025, pp. 432–437. doi: 10.1007/978-981-97-8313-7_60.
[66] Regional Agency for Environmental Protection of Piedmont (ARPA Piemonte), "https://www.arpa.piemonte.it/".
[67] R. Rahif, M. Hamdy, S. Homaei, C. Zhang, P. Holzer, S. Attia, Simulation-based framework to evaluate resistivity of cooling strategies in buildings against overheating impact of climate change, Build. Env. 208 (2022) 108599.
[68] C.R. Schwalm, S. Glendon, P.B. Duffy, RCP8. 5 tracks cumulative CO2 emissions, Proc. Natl. Acad. Sci. 117 (33) (2020) 19656–19657.
[69] A. Machard, et al., Typical and extreme weather datasets for studying the resilience of buildings to climate change and heatwaves, Sci. Data 11 (1) (May 2024) 531, https://doi.org/10.1038/s41597-024-03319-8.
[70] S. Yin, D. Chen, Weather generators. Oxford Research Encyclopedia of Climate Science, Oxford University Press, 2020, https://doi.org/10.1093/acrefore/9780190228620.013.768.
[71] M. Heiranipour, F. Favoino, M.J. Gutierrez, S. Avesani, Typical and extreme (heatwave) future weather files for building energy simulations: case studies for Turin and Bolzano, Italy, and De Bilt, Netherlands, Zenodo (Dec. 2024), https://doi.org/10.5281/zenodo.14274362.
[72] J.S. Haberl, D.E. Claridge, and C. Culp, "ASHRAE's guideline 14-2002 for measurement of energy and demand savings: how to determine what was really saved by the retrofit," 2005.
[73] C.J. Willmott, S.M. Robeson, K. Matsuura, A refined index of model performance, Int. J. Climatol. 32 (13) (2012) 2088–2094.
[74] S.E. Perkins, A.J. Pitman, N.J. Holbrook, J. McAneney, Evaluation of the AR4 climate models' simulated daily maximum temperature, minimum temperature, and precipitation over Australia using probability density functions, J. Clim. 20 (17) (2007) 4356–4376.
[75] R. Tällberg, B.P. Jelle, R. Loonen, T. Gao, M. Hamdy, Comparison of the energy saving potential of adaptive and controllable smart windows: a state-of-the-art review and simulation studies of thermochromic, photochromic and electrochromic technologies, Sol. Energy Mater. Sol. Cells 200 (Sep. 2019) 109828, https://doi.org/10.1016/j.solmat.2019.02.041.
[76] J.L.M. Hensen, R. Loonen, and S. Kin, "Building performance evaluation of integrated transparent photovoltaic blind system by a virtual testbed," 2014.
[77] R.C.G.M. Loonen, S. Singaravel, M. Trčka, D. Cóstola, J.L.M. Hensen, Simulation-based support for product development of innovative building envelope components, Autom. Constr. 45 (Sep. 2014) 86–95, https://doi.org/10.1016/j.autcon.2014.05.008.
[78] J. Neymark, et al., Update of ASHRAE Standard 140 Section 5.2 and Related Sections (BESTEST Building Thermal Fabric Test Cases), Argonne National Lab. (ANL), Argonne, IL (United States), 2020.
[79] A. Fundamentals, "ASHRAE Handbook 2017 Fundamentals SI; 2017," 2017.
[80] ISO 18523-1: Energy Performance of Buildings — Schedule and Condition of Building, Zone and Space Usage For Energy Calculation — Part 1, ISO, 2016.
[81] ISO 17772-1: Energy Performance of Buildings—Indoor Environmental Quality—Part 1: Indoor Environmental Input Parameters For the Design and Assessment of Energy Performance of Buildings Performance Geneva, ISO, Switzerland, 2017.
[82] E. Cen, 12464-1: 2002 Light and lighting—Lighting of work places–Part 1: indoor work places, Bruss. Belg. (2002).
[83] C. E. N. – E. C, For Standardization, *EN 14825 – Air conditioners, Liquid Chilling Packages and Heat pumps, With Electrically Driven compressors, For Space Heating and Cooling – Testing and Rating At Part Load Conditions and Calculation of Seasonal Performance*, CEN – European Committee for Standardization, 2012.
[84] Energy Performance of Buildings – Ventilation for Buildings – Part 7: Calculation methods For the Determination of Air Flow Rates in Buildings Including Infiltration (Module M5-5), European Committee for Standardization, Brussels, 2017.
[85] Applicazione Delle Metodologie Di Calcolo Delle Prestazioni Energetiche e Definizione Delle Prescrizioni e Dei Requisiti Minimi Degli Edifici, Ministero dello Sviluppo Economico, Dec. 2015 [Online]. Available, https://www.gazzettaufficiale.it.
[86] M.S. Roudsari and M. Pak, "Ladybug: a parametric environmental plugin for grasshopper to help designers create an environmentally-conscious design," 2013.
[87] U. S. D. of Energy, EnergyPlus Version 9.2. 0 Documentation. Engineering reference, US Department of Energy Washington, DC, USA, 2020.
[88] A. Olsson, G. Sandberg, O. Dahlblom, On Latin hypercube sampling for structural reliability analysis, Struct. Saf. 25 (1) (Jan. 2003) 47–68, https://doi.org/10.1016/S0167-4730(02)00039-5.
[89] L. Pérez-Lombard, J. Ortiz, R. González, I.R. Maestre, A review of benchmarking, rating and labelling concepts within the framework of building energy certification schemes, Energy Build. 41 (3) (Mar. 2009) 272–278, https://doi.org/10.1016/j.enbuild.2008.10.004.
[90] M. Santamouris, Cooling the buildings – past, present and future, Energy Build. 128 (Sep. 2016) 617–638, https://doi.org/10.1016/j.enbuild.2016.07.034.
[91] M. Hamdy, S. Carlucci, P.-J. Hoes, J.L.M. Hensen, The impact of climate change on the overheating risk in dwellings—A Dutch case study, Build. Env. 122 (Sep. 2017) 307–323, https://doi.org/10.1016/j.buildenv.2017.06.031.
[92] T. Hong, M. Ferrando, X. Luo, F. Causone, Modeling and analysis of heat emissions from buildings to ambient air, Appl. Energy 277 (Nov. 2020) 115566, https://doi.org/10.1016/j.apenergy.2020.115566.
[93] J.C. Helton, F.J. Davis, J.D. Johnson, A comparison of uncertainty and sensitivity analysis results obtained with random and latin hypercube sampling, Reliab. Eng. Syst. Saf. 89 (3) (Sep. 2005) 305–330, https://doi.org/10.1016/j.ress.2004.09.006.
[94] I. Sobol, "Sensitivity estimates for nonlinear mathematical models. Mathematical modeling and computational experiment," *vol*, vol. 1, pp. 407–414, 1993.
[95] R.E. Caflisch, Monte carlo and quasi-monte carlo methods, Acta Numer. 7 (1998) 1–49.
[96] G. Glen, K. Isaacs, Estimating sobol sensitivity indices using correlations, Environ. Model. Softw. 37 (Nov. 2012) 157–166, https://doi.org/10.1016/j.envsoft.2012.03.014.
[97] F. Giorgi, W.J. Gutowski, Regional dynamical downscaling and the CORDEX initiative, Annu. Rev. Env. Resour. 40 (1) (Nov. 2015) 467–490, https://doi.org/10.1146/annurev-environ-102014-021217.

[98] D. Jacob, et al., EURO-CORDEX: new high-resolution climate change projections for European impact research, Reg. Env. Change 14 (2) (Apr. 2014) 563–578, https://doi.org/10.1007/s10113-013-0499-2.
[99] M. Rummukainen, State-of-the-art with regional climate models, WIREs Clim. Change 1 (1) (Jan. 2010) 82–96, https://doi.org/10.1002/wcc.8.
[100] D. Maraun, Bias correcting climate change simulations - a critical review, Curr. Clim. Change Rep. 2 (4) (Dec. 2016) 211–220, https://doi.org/10.1007/s40641-016-0050-x.
[101] J. Remund, S. Müller, C. Schilter, B. Rihm, The use of Meteonorm weather generator for climate change studies, EMS Annu. Meet. Abstr. 7 (Sep. 2010).
[102] M.F. Jentsch, P.A.B. James, L. Bourikas, A.S. Bahaj, Transforming existing weather data for worldwide locations to enable energy and building performance simulation under future climates, Renew. Energy 55 (2013) 514–524.
[103] A. Sehizadeh, H. Ge, Impact of future climates on the durability of typical residential wall assemblies retrofitted to the PassiveHaus for the Eastern Canada region, Build. Env. 97 (2016) 111–125.
[104] L. Wang, X. Liu, H. Brown, Prediction of the impacts of climate change on energy consumption for a medium-size office building with two climate models, Energy Build. 157 (Dec. 2017) 218–226, https://doi.org/10.1016/j.enbuild.2017.01.007.
[105] S. Schroderus, J. Havelka, A. Kouch, K. Illikainen, S. Alitalo, F. Fedorik, Hygrothermal performance of hybrid multi-storey buildings under future climate scenarios, Appl. Therm. Eng. 259 (Jan. 2025) 124917, https://doi.org/10.1016/j.applthermaleng.2024.124917.